Optimizing the Stacking Moiety and Linker of 2′-Acylamido Caps of DNA Duplexes with 3′-Terminal Adenine Residues

Michael Printz and Clemens Richert*

Institute for Organic Chemistry, University of Karlsruhe (TH), 76131 Karlsruhe, Germany

Received October 14, 2006

Reported here is the synthesis of oligodeoxynucleotides with a 3′-terminal 2′-acylamido-2′-deoxyadenosine residue. The route to these oligonucleotides employs an *N,O*-Alloc-protected 5′-phosphoramidite of 2′-amino-2′-deoxyadenosine that was prepared in 11 steps from arabinoadenosine. Small combinatorial libraries of oligonucleotides were generated via acylation with a mixture of linker amino acids and subsequent acylation of their amino groups. Mass spectrometrically monitored nuclease selection assays led to oligonucleotides whose 2′-substituent increases the thermal stability of the DNA duplexes. A linker with three methylene groups between a perylene stacking moiety and the amido group gives a UV-melting point increase of up to 27.9 °C for the DNA sequence $(TGCGCA^*)_2$, where A* denotes the 2′-acylamidoadenosine residue. The same acylamido group improves mismatch discrimination at the terminal position with a melting point depression of ≥7 °C for any of the three mismatches in the target sequence of the octamer 5′-AGGTTGAA-3′. These results demonstrate how even a very weakly base-pairing nucleotide at the 3′-terminus of a DNA probe strand can be enforced to engage in strong and highly sequence-selective base-pairing interactions.

Introduction

Three modes of interaction dominate our perception of how small molecules can bind to double-stranded DNA: intercalation, groove binding, and electrostatic binding to the backbone. A fourth mode of binding, namely, stacking on the terminal base pair of DNA, RNA, or hybrid helices, is only beginning to emerge. This fourth mode of binding has been demonstrated for small molecules covalently linked to one or both strands of a duplex.[1,2,3] The covalently appended small molecule ligands can act as molecular "caps", bridging the two strands in a way that can suppress fraying at the terminus. As a result, caps, when appended to immobilized DNA strands, can improve target affinity and base-pairing fidelity of hybridization probes, including the probe strands on DNA microarrays.[4,5,6] High-fidelity base pairing throughout the length of a duplex is critical for microarray experiments,[7] where many closely related sequences may compete for binding the immobilized strands, leading to false positive signals, unless hybridization to mismatched probe strands is suppressed.[8]

We have previously performed combinatorial studies on caps attached to the 5′-terminus of oligonucleotides.[9,10a,b11b] Our search for caps covalently linked to the 3′-terminal residue of a DNA strand has been limited to ligands attached to (deoxy)uridine at this terminus. Even for oligonucleotides with terminal uridines, no more than exploratory combinatorial work has been performed.[12] Further, our first duplex-stabilizing 2′-acylamido substituent of uridine, the residue of nalidixic acid, initially believed to act as a true cap,[13] was later shown to disrupt the terminal base pair.[14] Also, the lead identified in our exploratory combinatorial work, the residue of anthraquinone carboxylic acid, gives relatively poor base-pairing fidelity at the terminus,[12] as well as relatively broad melting transitions.

In the current study, we turned our attention to possible caps for (deoxy)adenosine as a terminal nucleoside. The improvement of base-pairing fidelity through capping is desirable for adenine and uracil/thymine as terminal nucleobases because they form weak base pairs with just two hydrogen bonds, further compounding the already poor selectivity at the end of the helix. Between the two, adenine at the terminus is the most difficult case.[11b] A cap attached to an adenosine residue will face a small (pyrimidine) ring of uracil/thymine in the target strand, with which it has to engage in strong enough stacking interactions to exert a significant duplex-stabilizing effect. We decided to append the stacking moieties to the 2′-position of the 3′-terminal adenosine residue of oligodeoxynucleotides (Figure 1). The 2′-position is well suited for attaching such stacking moieties, as this leaves the 3′-position free for attachment to the surface of microarrays[6] and does not block Watson−Crick base pairing, as documented for DNA and RNA derivatives featuring 2′-substituents.[15,16,17]

There is a range of possible stacking moieties known from the literature, including residues of cholic acid,[18] pyrene,[19] dipyridophenanzine,[20] phenanthrene,[21] stilbene,[5,22] perylene,[23] certain porphyrins,[24] anthraquinone,[11] and ethidium,[25] not to mention dangling (*C*)-nucleosidic residues[26] or dangling nucleobase analogs in general.[27] We therefore felt compelled to launch a small combinatorial study to find a suitable cap for DNA duplexes terminated in a 2′-acylamido-2′-deoxyadenosine residue, as well as a linker that properly positions the cap for stacking on the terminal base pair with a

* To whom correspondence should be addressed. Phone: 49 (0) 721 608 2091. Fax: 49 (0) 721 608 4825. E-mail: cr@rrg.uka.de.

10.1021/cc060142a CCC: $37.00
Published on Web 02/01/2007

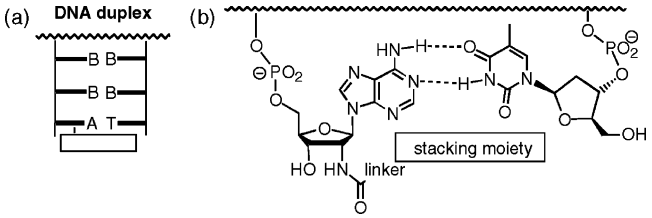

Figure 1. (a) Schematic and (b) general structure of duplex with 2′-acylamidoadenosine residue.

thymidine residue in the target strand. To search a useful portion of cap and linker structure space, we decided to expand on our methodology of producing small combinatorial libraries through on-support acylation and to select from these libraries through mass spectrometrically monitored nuclease selection,[10a,c,12,11b] a technology developed to rapidly screen small chemsets of modified oligonucleotides without the need to purify individual compounds. It was hoped that the results would also shed some light on the more general question of how ligands interact with DNA through stacking.

Results

Oligonucleotides with 3′-terminal 2′-amino-2′-deoxyadenosine residues (Figure 1) were the target molecules of our syntheses. The assembly of such oligonucleotides can be achieved with phosphoramidite building blocks suitable for automated DNA synthesis. We chose 5′-phosphoramidite **1** as such a building block (Scheme 1) because a 5′ → 3′ chain assembly ensures that the residue to be acylated resides at the distal position of the DNA chain. This makes this residue sterically more accessible than a residue proximal to the solid support, and it allows for acylation as the last step of the solid-phase syntheses. Conventional, 3′ → 5′ synthesis would require that acylation either be performed on a sterically hindered proximal residue or that the acyl groups introduced do not possess functional groups that are reactive toward phosphoramidites (in case one was to perform chain assembly after acylation). Allyloxycarbonyl (Alloc) protecting groups were deemed suitable for the protection of the 2′-amino group and the neighboring 3′-hydroxy group of the nucleoside. This carbamate/carbonate protecting group is orthogonal to the silyl protecting groups envisioned for the early steps of the synthesis, survives the coupling and oxidation steps of automated DNA synthesis, and is removable in the presence of other DNA-protecting groups, as well as the succinyl linker to controlled pore glass (cpg).[28]

Our synthesis of **1** started from arabinofuranosyladenosine **2**, which was converted to azide **3**[29] in 75% yield over 3 steps, using the route of Karpeisky and colleagues.[30] Similar routes involving inversion at C2 of adenosine[31] or arabinoadenosine[32] via S_N2 displacement are known and were not explored. The addition of benzoyl chloride to **3** and the subsequent treatment with morpholine to convert overacylated side products,[32] gave **4** in a 90% yield. Reduction of the azido group to amine **5** was achieved by hydrogenation with Pd/C in a near-quantitative yield. The free amine was immediately protected to give **6**, avoiding handling very polar intermediates. Unexpectedly, attempts to install the Alloc group with Alloc chloride gave low yields (52%). The use of the *N*-hydroxysuccinimide instead of the chloride improved the yield to 64%, but the best results were obtained when the hydroxybenzotriazolide of Alloc was used (72%). The latter reagent is also less toxic than Alloc-Cl. Desilylation to **7** proceeded uneventfully when TBAF in THF was used (91%).

Initially, we tried to generate a 5′-phosphoramidite without prior protection/deprotection of the 5′-position. All attempts to convert **7** to an *N*2′,*O*3′-acetonide, analogous to that reported for aminodeoxyuridine,[11b] failed. When forcing conditions were employed (H_2SO_4 or CSA as catalyst), depurination occurred. Consequently, we installed a dimethoxy-

Scheme 1. Synthesis of Phosphoramidite **1**[a]

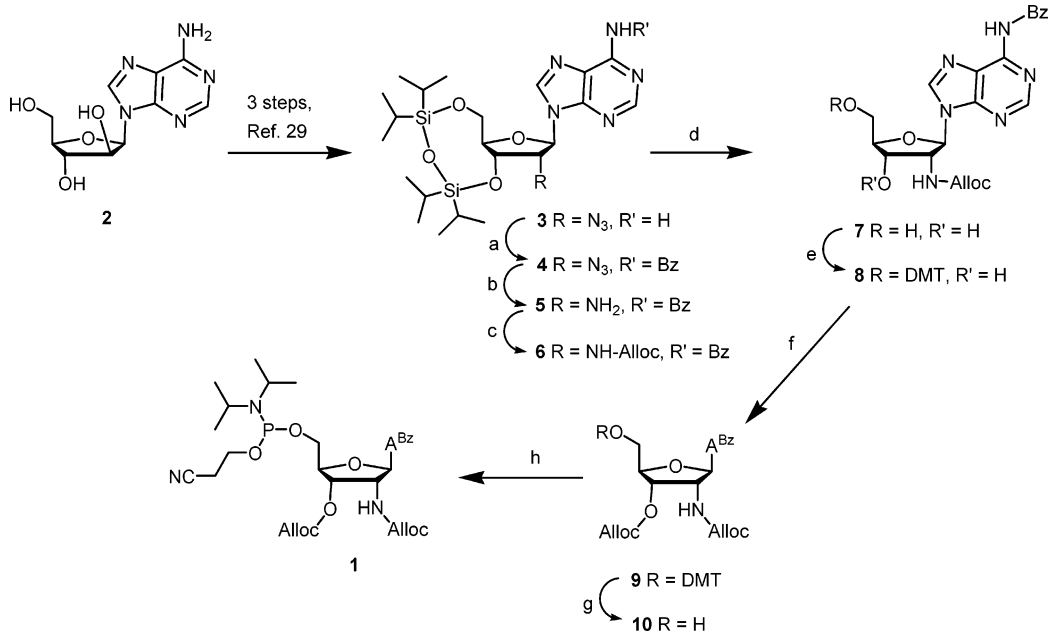

[a] Conditions : (a) (1) BzCl, pyridine, (2) morpholine, 90%; (b) Pd/C, H_2, MeOH, 99%; (c) Alloc-OBt, pyridine, 72%; (d) TBAF, THF, 91%; (e) DMTCl, pyridine, DMAP, 85%; (f) Alloc-OAt, pyridine 72%; (g) TFA, H_2O, CH_2Cl_2, 90%; (h) (iPr$_2$N)P(OCH$_2$CH$_2$CN)Cl, DIEA, MeCN, 84%.

Scheme 2. Synthesis of Oligonucleotides[a]

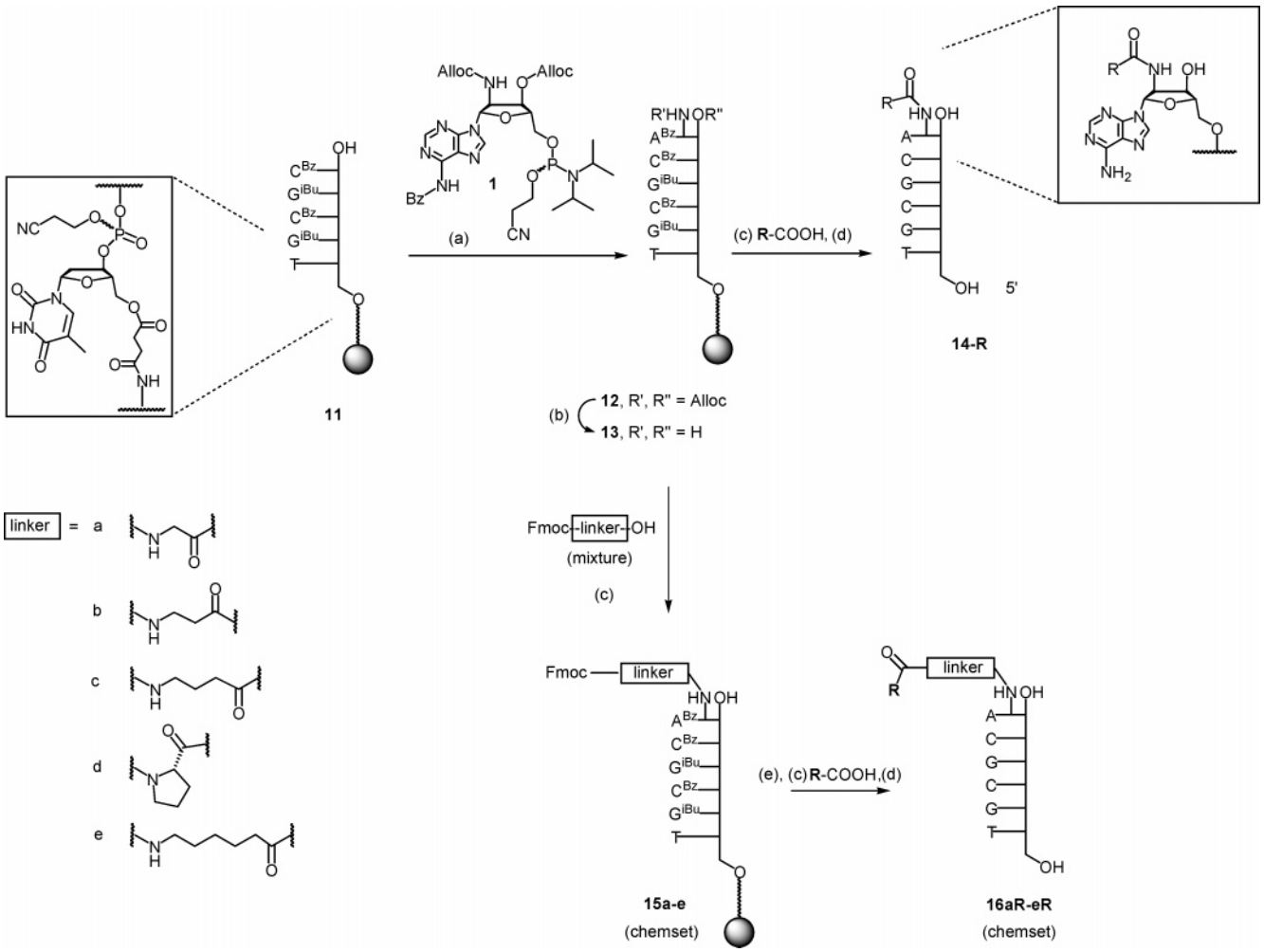

[a] (a) Chain elongation cycle with phosphoramidite **1**; (b) $[Pd(PPh_3)_4]$, PPh_3, $[Et_2NH_2]^+$ $[HCO_3]^-$, CH_2Cl_2; (c) HATU, HOAt, DIEA, DMF; (d) NH_4OH; (e) piperidine, DMF.

trityl group at the 5′-position (**8**, 85%), protected the remaining 3′-hydroxyl group with another Alloc moiety (**9**, 72%), and detritylated **9** to obtain **10** (90%). Phosphitylation of **10** provided **1** in an 84% yield after column chromatography. The 11 step synthesis of **1** from **2** proceeds in 30% overall yield and has been performed repeatedly with gram quantities.

Scheme 2 shows our synthetic route to oligonucleotides. Phosphoramidite **1** was coupled to the 5′-terminal portion of the DNA sequence (**11**), which had been assembled using commercial 5′-phosphoramidites.[33] Not surprisingly, analytical samples of **12**, when deprotected with aqueous ammonia and analyzed by MALDI-TOF mass spectrometry, gave a signal whose mass was 28 Da higher than that of the free amino alcohol. Most probably, the carbonate is cleaved first, giving a free 3′-hydroxy group that then displaces the allyl alcohol in the neighboring 2′-carbamate. Double-Alloc deprotection with $Pd[PPh_3]_4$ and diethylammonium bicarbonate gave **13** in a high yield, as shown by mass spectra of the crudes obtained through deprotection with NH_4OH. Solid support-bound **13** was then used for acylation, either to give directly coupled acyl groups (**14-R**), or to provide oligonucleotides with a linker amino acid residue (via **15a**−**e**). Compared to coupling reactions involving 2′-amino-2′-deoxyuridine as the 3′-terminal residue,[12] these reactions were found to be unusually low yielding. Even when unhindered carboxylic acids, such as indole propionic acid, were reacted, no more than 50% conversion was found, with the usual[34] activation with HBTU/HOBt and more than 100 equiv of active ester, as seen in MALDI spectra of crudes. This forced us to use more reactive esters, generated with HATU[35]/HOAt, and elevated temperatures, either produced by microwave irradiation or an oil bath. The reaction with OAt esters at 50 °C for 30 min gave near-quantitative acylation of the 2′-amine, as detected in MALDI spectra of the crudes after basic deprotection. (We assume that the 3′-hydroxyl group also undergoes acylation under these conditions and that the resulting ester is cleaved during the deprotection step with ammonium hydroxide.)

With the synthetic route established, we next sought to identify 2′-substituents that increase the thermal stability of DNA duplexes. As mentioned above, we wished to search both for stacking moieties and the linker connecting them to the 2′-position of the terminal adenosine residue. Our preferred combinatorial methodology involves the synthesis of small combinatorial libraries of acylated oligonucleotides and mass spectrometrically monitored selection assays. In the past, we have usually performed mixed coupling reactions with several activated carboxylic acids as the penultimate step of our solid-phase syntheses, followed by a single

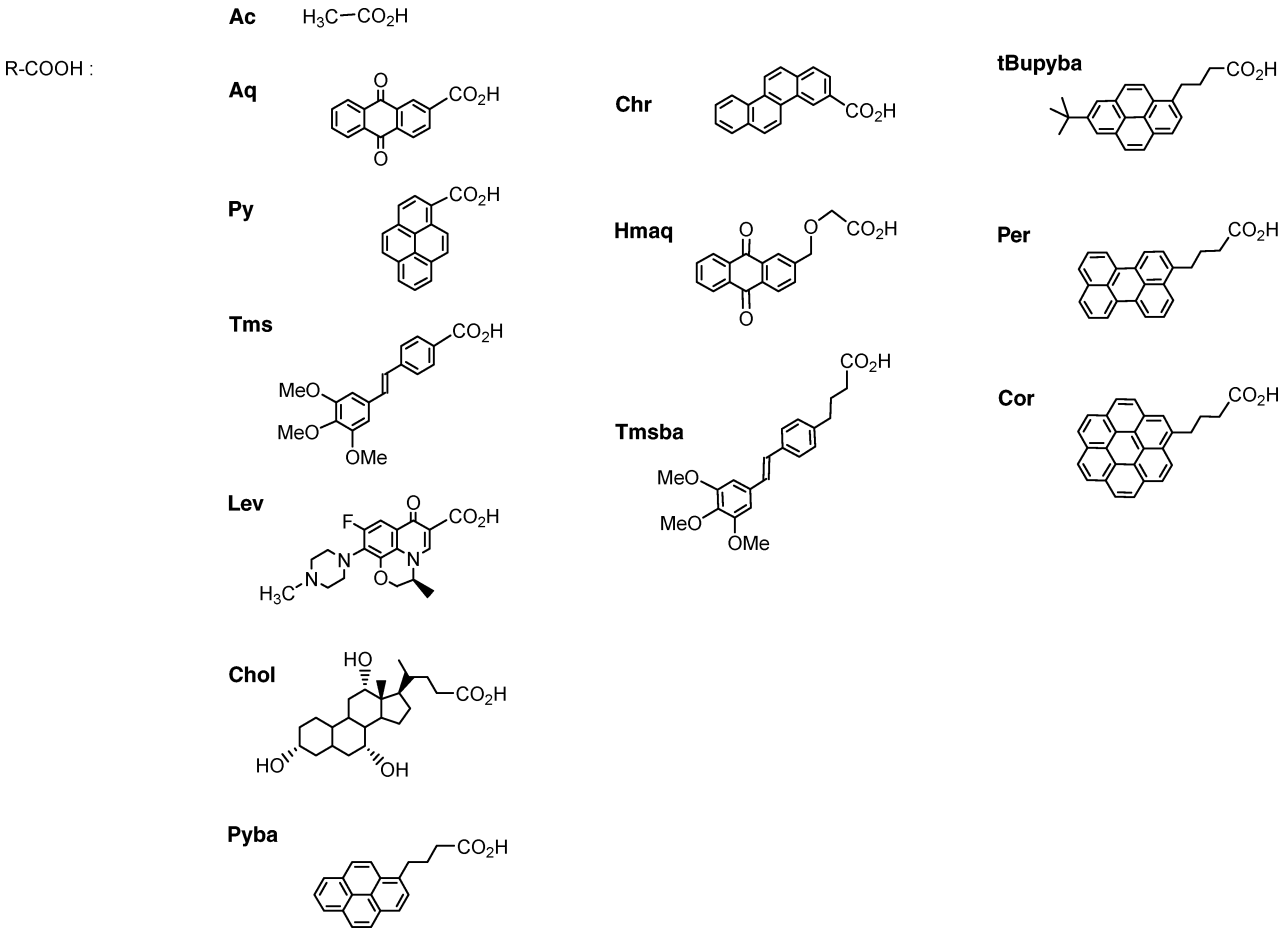

Figure 2. Structures of carboxylic acids employed.

deprotection step, releasing the library members from the support.[12,10a−f] In the current study, we decided to perform mixed coupling reactions with five amino acid linkers that differ in their alkyl portion. This has the advantage of having to evolve a reactivity-adjusted mixture[10d] only once. The acylation with carboxylic acids featuring the stacking moieties then occurs individually, without competition between structurally diverse building blocks.

A reactivity-adjusted coupling mixture containing the *N*-Fmoc-protected forms of glycine (a), β-alanine (b), γ-amino butyric acid (c), proline (d), and ϵ-amino hexanoic acid (e) was used to generate **15a**−**e** (Scheme 2). We obtained roughly equimolar quantities of each of the five acylated products, as detected in MALDI-TOF mass spectra of analytical samples deprotected with aqueous ammonia. Subsequent Fmoc-removal from the solid support-bound chains with piperidine and acylation of the resulting amines with one of the carboxylic acids shown in Figure 2 gave crude chemsets **16aR**−**eR** in high yields, as required for spectrometrically monitored selection assays.[36] The carboxylic acids chosen include a bile acid,[37] a quinolone,[38] anthraquinone,[12,39] a substituted stilbene,[5] and apolar aromatic compounds,[11b] which were hits in earlier combinatorial searches for moieties that can cap DNA duplexes. Further, all carboxylic acid building blocks have roughly the size of a terminal base pair, as required for the capping mode of binding envisioned for the 2′-acylamido groups.

Figure 3 shows the MALDI-TOF mass spectrum of a mixture produced by combination of the crude product of

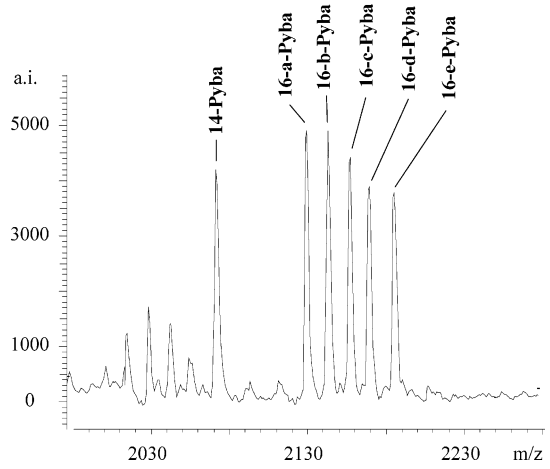

Figure 3. MALDI-TOF mass spectrum of a six component mixture of oligonucleotides **14-Pyba**, **16a-Pyba**, **16b-Pyba**, **16c-Pyba**, **16d-Pyba**, and **16e-Pyba**. The library portion (compounds of general structure **16**) was generated via the route shown in the lower part of Scheme 2. Compound **14-Pyba** was added separately.

library synthesis, as shown in the lower part of Scheme 2, and the one oligonucleotide whose acyl group is directly appended to the 2′-amino group of the 3′-terminal adenosine residue (**14-R**). Such mixtures were produced for each of the carboxylic acid building blocks shown in the first column of Figure 2. Nuclease selection assays were performed with these mixtures, providing the protection factors[10] listed in Table 1. The details of how one obtains protection factors from the kinetics of nuclease degradation of self-comple-

Table 1. Protection Factors[a] Obtained from Nuclease Survival Assays Involving Mixtures of DNA Hybrids of the Sequence 5′-TGCGCA-linker-R-3′

compound	PF[b]	$PF_{co+trunc}$[c]
14-Aq	2.9	3.7
16-a-Aq	3.0	4.2
16-b-Aq	4.2	8.7
16-c-Aq	3.4	5.0
16-d-Aq	2.9	4.0
16-e-Aq	1.8	1.8
14-Py	3.0	2.0
16-a-Py	3.7	2.7
16-b-Py	5.7	5.5
16-c-Py	3.7	2.7
16-d-Py	3.5	2.5
16-e-Py	3.8	2.5
14-Tms	1.5	1.4
16-a-Tms	3.7	5.6
16-b-Tms	4.2	6.8
16-c-Tms	3.4	4.8
16-d-Tms	2.4	2.4
16-e-Tms	2.2	2.4
14-Lev	1.4	1.7
16-a-Lev	1.1	1.2
16-b-Lev	0.8	0.6
16-c-Lev	1.4	1.6
16-d-Lev	0.7	0.5
16-e-Lev	1.0	1.0
14-Chol	4.7	4.9
16-a-Chol	1.7	1.6
16-b-Chol	2.5	2.4
16-c-Chol	1.2	1.1
16-d-Chol	3.0	2.9
16-e-Chol	1.1	1.0
14-Pyba	2.9	3.7
16-a-Pyba	1.6	1.7
16-b-Pyba	2.3	2.6
16-c-Pyba	1.4	1.4
16-d-Pyba	2.6	3.1
16-e-Pyba	1.1	0.9
14-Ac (control)	1.0	1.0

[a] See ref 10a for the definition of protection factors. [b] Protection factor. [c] Protection factor with cutoff and truncation at 20%.

mentary oligonucleotides are given in ref 10a. Suffice it to say that the process is based on the integration of the area under the data points for the kinetics of the disappearance of full-length oligomers upon nuclease digestion relative to that of a reference compound and that the higher the protection factor, the more likely that a duplex of increased stability is formed by the acylated oligonucleotide. To achieve baseline resolution between peaks, all MALDI-TOF mass spectra were acquired in the reflectron mode of the spectrometer.

Representative spectra from a nuclease selection, involving oligonucleotides featuring the residue of cholic acid, are shown in Figure 4. It can be discerned that the relative intensity of the peak for linker-free oligonucleotide **14-Chol** increases toward the end of the assay, leading to the highest nuclease protection factor against acetylated control compound **14-Ac** among the components of this mixture. The structure−activity map obtained from our nuclease assays reveals a clear trend. For building blocks **Py**, **Tms**, and **Aq**, whose carboxylic acid function is directly linked to the ring system, a β-alanine linker (**b**) gives the highest protection factor (PF) values (Table 1). For building blocks **Chol** and

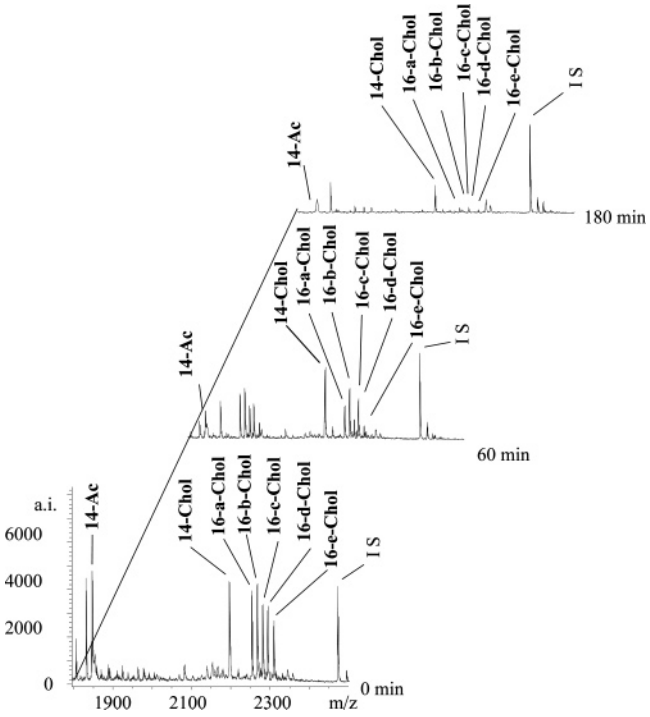

Figure 4. MALDI-TOF mass spectra from samples drawn during nuclease survival selection from the mixture of **14-Ac**, **16-Chol**, **16-a-Chol**, **16-b-Chol**, **16-c-Chol**, **16-d-Chol**, and **16-e-Chol.** Peaks of the full length oligonucleotides are labeled: IS = internal standard. Toward the end of the selection, the peak for linker-free **16-Chol** shows the greatest relative intensity, identifying this compound as the winner of the assay.

Pyba with a "built-in" alkyl linker between carboxylic acid function and the ring system, the optimum in structure space is the compound without an additional linker. Only for levofloxacin (**Lev**), similar protection factors were observed for the oligonucleotide with a β-alanine linker and the one lacking a linker. It is known that quinolones can disrupt base pairs upon binding to DNA,[38,14] so this "unusual" behavior of the quinolone levofloxacin was not surprising. In conclusion, except for **Lev**, the linker chain between the ring system and the 2′-position of the adenosine (built-in or installed) that gave the optimum in protection factors was five centers long, including the amide.

A total of 14 oligonucleotides with high protection factors were resynthesized individually, HPLC purified, and subjected to melting point experiments at three different salt concentrations (Table 2). As expected, the protection factors, which rely on the kinetic read-out of binding equilibria involving homo- and heteroduplexes, do not strictly correlate with UV melting-point increases measured for individual compounds. Still, among the oligonucleotides with the same stacking moiety, the order of activity established in the nuclease selections was confirmed. The oligonucleotide with the highest duplex melting point in this group was **14-Pyba**. The duplex $(\mathbf{14\text{-}Pyba})_2$ melts between 24.1 and 25 °C higher than that of unmodified $(TCGCGA)_2$. Also, the hyperchromicity observed for the dissociation of the former duplex is almost twice that of the control duplex.

Four other acylated oligonucleotides subjected to melting curve analysis gave T_m values within 6 °C of the value found for $(\mathbf{14\text{-}Pyba})_2$, including anthraquinone-bearing **16-b-Aq** and

Table 2. UV-Melting Points and Hyperchromicities Accompanying Duplex Dissociation for Self-Complementary DNA Hexamers of the Sequence 5′-TGCGCA-3′ with or without a 3′-Terminal 2′-Acylamido-2′-deoxyadenosine Residue[a]

	T_m at [NaCl] (°C)			hyper-chromicity (%)[b]
compound	none	150 mM	1 M	
TGCGCA (control)	23.2 ± 0.6	33.8 ± 0.8	34.3 ± 1.4	9.0 ± 2.0
14-Aq	35.9 ± 0.5	47.8 ± 0.2	50.2 ± 0.4	14.0 ± 1.0
16-b-Aq	42.6 ± 0.5	52.3 ± 0.3	55.1 ± 0.7	11.0 ± 1.5
16-c-Aq	42.2 ± 0.4	52.2 ± 0.2	54.1 ± 0.6	13.1 ± 1.4
16-d-Aq	37.2 ± 0.3	48.1 ± 0.1	49.9 ± 0.3	10.3 ± 0.7
16-b-Py	36.0 ± 1.0	47.7 ± 0.4	50.3 ± 0.4	16.0 ± 1.0
16-b-Tms	38.2 ± 0.5	48.0 ± 0.4	50.0 ± 0.3	16.0 ± 0.8
16-c-Lev	38.0 ± 0.3	46.3 ± 0.1	47.6 ± 0.3	14.4 ± 0.8
16-e-Lev	35.0 ± 0.4	44.0 ± 0.2	45.9 ± 0.5	14.0 ± 1.0
14-Chol	42.7 ± 0.3	52.0 ± 0.1	54.1 ± 0.2	14.7 ± 0.7
16-b-Chol	37.9 ± 0.5	47.8 ± 0.2	49.5 ± 0.4	13.3 ± 1.0
16-d-Chol	39.1 ± 0.4	48.5 ± 0.2	50.4 ± 0.3	15.0 ± 1.0
14-Pyba	47.9 ± 0.3	57.9 ± 0.2	59.3 ± 0.4	17.4 ± 0.9
16-b-Pyba	39.6 ± 0.2	50.4 ± 0.4	52.3 ± 0.2	15.1 ± 0.5
16-d-Pyba	42.4 ± 0.4	52.9 ± 0.2	55.8 ± 0.4	12.0 ± 0.9
16-b-Chr	*c*	56.5 ± 0.6	57.8 ± 0.5	10.0 ± 2.0
16-c-Chr	*c*	*c*	*c*	
16-d-Chr	41.1 ± 0.2	48.0 ± 2.0	48.7 ± 0.5	9.7 ± 1.0
17	21.2 ± 0.8	34.9 ± 1.5	37.9 ± 0.6	9.0 ± 0.5
14-Hmaq	41.3 ± 0.6	51.0 ± 0.3	52.4 ± 0.4	15.0 ± 2.0
14-Tmsba	44.0 ± 0.5	53.1 ± 0.4	54.4 ± 0.7	17.9 ± 0.9
14-tBupyba	47.2 ± 0.3	56.9 ± 0.2	58.7 ± 0.3	17.1 ± 1.8
14-Cor	49.2 ± 0.7	58.6 ± 0.8	58.4 ± 1.7	18.0 ± 3.0
14-Per	50.7 ± 0.2	60.5 ± 0.3	62.2 ± 0.2	23.4 ± 1.4

[a] Conditions: 4 μM strand concentration, 10 mM sodium phosphate buffer, pH 7.0, and NaCl concentration given. [b] Hyperchromicity between low- and high-temperature baseline at 260 nm for 1 M NaCl. [c] No melting point, not sufficiently cooperative transition.

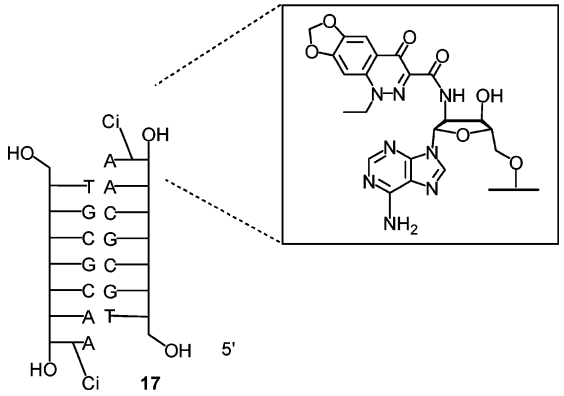

Figure 5. Structure of a duplex formed of heptamer **17** featuring a composite cap of a dangling adenosine residue with a 2′-amide-linked cinnoxacin residue.

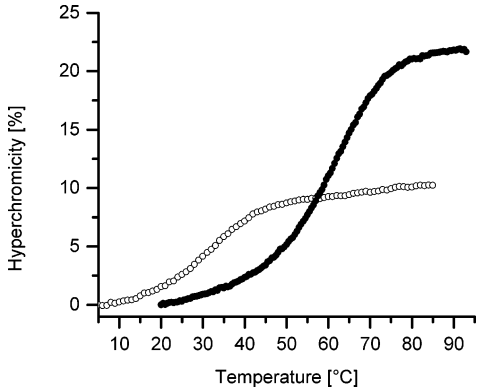

Figure 6. Melting curves of $(TGCGCA)_2$ (○) and $(\mathbf{14\text{-}Per})_2$ (●) at 4 μM strand concentration, 10 mM phosphate buffer pH 7.0, and 1 M NaCl.

16-c-Aq, cholic acid-bearing **14-Chol**, and linker-containing pyrenyl derivative **16-d-Pyba**. Another five oligonucleotides gave melting points above 50 °C, that is, within 9.3 °C of the value for $(\mathbf{14\text{-}Pyba})_2$, including stilbene derivative **16-b-Tms** and **16-b-Py** featuring the residue of pyrene carboxylic acid. As a consequence, a number of individual compounds were then prepared to probe the structure space for an optimum not discovered with the oligonucleotides contained in the mixtures used for selection assays.

First, we probed whether a structural isomer of pyrene could fit the binding site at the terminus of the DNA duplex better. We had speculated in our earlier work that chrysene could be a stacking partner for termini of DNA duplexes.[40] So, chrysene carboxylic acid (**Chr**) was prepared (Figure 2) following a literature protocol.[41] The NMR-spectroscopic data for **Chr** suggested that we obtained chrysene-3-carboxylic acid[42] as the only isomer. The UV-melting analysis of the DNA hybrid **16-b-Chr**, featuring the residue of this chrysene carboxylic acid, did give a higher melting point than that of **16-b-Py**, but a broad transition was observed at low salt concentration, and the highest melting point measured, at 1 M NaCl, was below that of $(\mathbf{14\text{-}Pyba})_2$ under these conditions. Two other derivatives of chrysene, **16-c-Chr** and **16-d-Chr**, differing in the nature of the linker, did not give more favorable results (Table 2), so that chrysenyl caps were not pursued further.

Next, we tested alternative steroid-DNA hybrids. Attempts were made to attach lithocholic acid methyl ester and cholesterol via carbamate linkers to the 2′-amino group of the terminal adenosine residue. For this, chloroformates were reacted with solid support-bound **13** in the presence of diisopropyl ethylamine. Unfortunately, degradation of the DNA chain was observed after deprotection, as well as loss of DNA chains from the support, even when commercial cholesteryl chloroformate was used as reagent. Further, two peaks giving the correct product mass were observed in HPLC traces of crudes. Exploratory experiments gave melting points below those of the control duplex for either of the fractions, so that no further attempts were made to prepare hybrids with a linkage between the A-ring of a steroid and the DNA.

We also prepared compound **17** (Figure 5), which features a cinoxacin residue linked to A6 of the core hexamer through a dangling aminodeoxyadenosine residue as linker. We chose to test this linker construct for the quinolone because exploratory work performed in the context of DNA duplexes with a 3′-terminal 2′-acylamido-2′-deoxyuridine residue suggested that such a "composite cap" might be superior to those directly linked to the 2′-position of the deoxyuridine residue.[14] In the event, the duplex of compound **17**, though

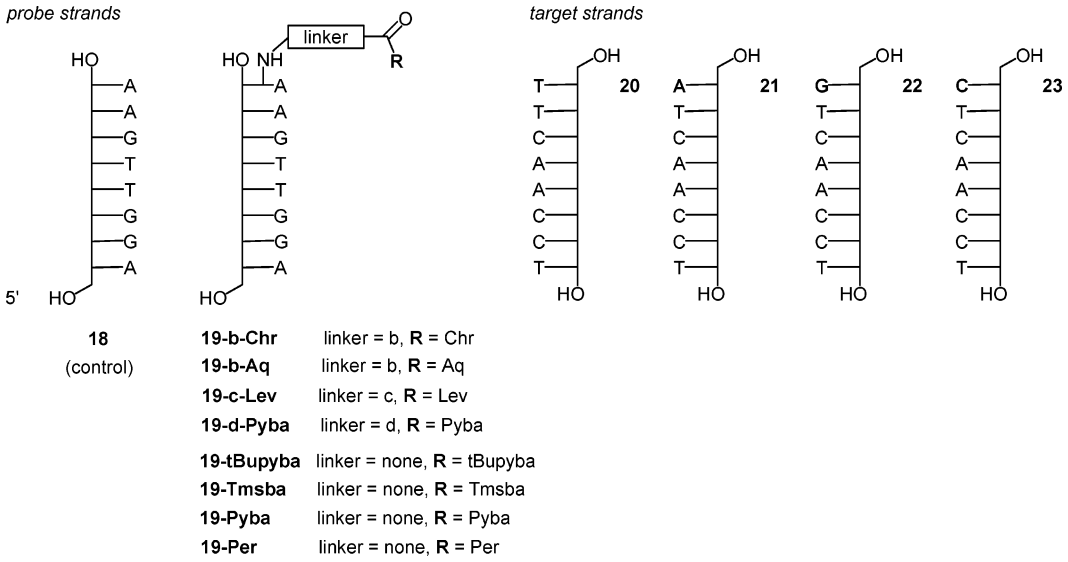

Figure 7. Octamer sequences employed in studies on mismatch discrimination at the terminus.

superior in thermal stability to the unmodified control at high salt concentration, gave lower melting points than most of the other hexamers tested (Table 2).

We then turned to preparing derivatives of anthraquinone and trimethoxystilbene that feature a linker of the same length and flexibility as pyrene butyric acid (**Pyba**), our lead structure from the nuclease selection assays. Two carboxylic acids with flexible three-atom linkers between the aromatic ring system and carboxylic acid group (Figure 2) were prepared (see Scheme S1, Supporting Information). One of these is a stilbene, namely, (*E*) 4-[4-(3,4,5-trimethoxystyryl)-phenyl]butanoic acid (**Tmsba**), prepared in two steps from a literature-known Wittig salt (**24**, Supporting Information) and trimethoxybenzaldehyde.[43] Further, anthraquinone derivative 2-[(anthraquinone-2-yl)methoxy]acetic acid (**Hmaq**) was synthesized in 2 steps, starting from 2-(bromomethyl)-anthraquinone (**27**)[44] (see Supporting Information). Either of these flexibly tethered carboxylic acids was coupled to **13**, followed by deprotection, and the hybrids were subjected to UV-melting analysis (Table 2). Gratifyingly, the melting points of stilbene-containing hybrid (**14-Tmsba**) were found to be higher than those of the **16-b-Tms** with its more rigid linker containing two amide functionalities. But, the melting transition of the duplex (**14-Hmaq**)$_2$ was rather broad, and the melting points determined did not exceed those measured for **16-b-Aq**.

Finally, derivatives of **14-Pyba** with expanded ring systems were prepared. First, a *tert*-butyl derivative of pyrene butyric acid (**tBupyba**) was prepared, under reaction conditions similar to those reported for alkylating methylpyrene.[45] We hoped that the bulky *tert*-butyl group would be able to engage in favorable van der Waals interactions with the DNA. The UV-melting points of the resulting DNA hybrid (**14-tBupyba**) were similar to those of **14-Pyba**, so any such interactions (if they were present) did not seem to have a significantly duplex-stabilizing effect. At last, perylene butyric acid[46] (**Per**) and coronene butyric acid[47] (**Cor**) with larger aromatic π-systems than pyrene were tested. The perylene-containing (**14-Per**)$_2$ did indeed show a melting point approximately 3 °C above that of (**14-Pyba**)$_2$ at any of the salt concentrations tested. The T_m increase over the control duplex (TGCGCA)$_2$ was between 26.7 and 27.9 °C, that is, the highest value found in the current study. Further, this large aromatic cap gave a relatively sharp melting curve with massively increased hyperchromicity at 260 nm (Figure 6). Caps linked to the 5′-terminus of oligonucleotides that improve duplex stability and mismatch discrimination also induce substantial increases in hyperchromicity at 260 nm,[37] though not to such an extent. Coronene derivative **14-Cor** gave a duplex-to-single strand transition considerably broader than that of either control duplex or (**14-Per**)$_2$. Also, the melting points measured for (**14-Cor**)$_2$ were below that of (**14-Per**)$_2$.

We then asked whether the perylene cap provides a selectivity-enhancing effect on base pairing at the terminus. For this, we synthesized non-self-complementary sequence 5′-AGGTTGAA-3′ and derivatives thereof with a 3′-terminal 2′-acylamidoadenosine residue (Figure 7). Duplexes with target strands **20**−**23**, differing in the 5′-terminal nucleobase were subjected to UV melting. Eight cap-bearing oligonucleotides were included in this part of the study to gain a broader perspective of how structure affects the fidelity of base pairing.

As expected for a weakly base-pairing adenine at the terminus of the duplex, neither of the three mismatched target strands induced a large decrease in the melting temperature for the unmodified control (ΔT_m < 4.5 °C). All duplexes with a cap gave substantially higher melting points for the perfectly matched duplex (up to 15.3 °C T_m increase) and improved mismatch discrimination, as evidenced by a greater drop in melting points in the presence of a target strand with mismatched nucleobase. Interestingly, this was also true for **19-c-Lev**, even though quinolones have a high propensity to disrupt weak terminal base pairs.[38,11b] Apparently, the lengthy γ-aminobutyric acid linker suppresses this disrupting effect in the present case. Four caps performed best in this sequence context, with melting points for the fully matched duplex ~15 °C above that of the control and within 0.4 °C

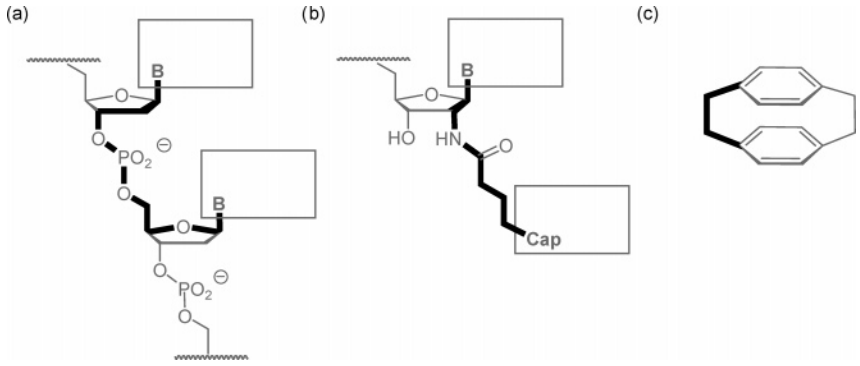

Figure 8. Comparison of the linkers between stacking partners of (a) a dinucleotide portion in a DNA duplex, (b) the terminal nucleotide and the cap appended to it via a linker found as optimal in this work, and (c) a paracyclophane, where two aromatic rings stacking on each other are connected by a very short linker.

Table 3. UV-Melting Points of DNA Hybrids 5′-AGGTTGAA-linker-R with Perfectly Matched (**20**), A-mismatched (**21**), G-mismatched (**22**), and C-mismatched (**23**) Target Strands[a]

	target strand			
probe strand	**20**	**21**	**22**	**23**
18	29.8 ± 0.3	27.0 ± 0.5	25.5 ± 0.4	25.5 ± 0.6
19-b-Chr	38.1 ± 0.6	33.4 ± 0.6	34.2 ± 0.5	29.8 ± 0.3
19-b-Aq	40.0 ± 0.4	34.1 ± 0.6	33.5 ± 0.5	28.8 ± 0.9
19-c-Lev	39.8 ± 0.3	33.1 ± 0.5	34.6 ± 0.3	27.2 ± 1.2
19-tBupyba	45.0 ± 0.4	37.0 ± 0.5	36.9 ± 0.4	32.5 ± 0.3
19-Tmsba	44.8 ± 0.5	33.5 ± 0.4	39.3 ± 0.5	29.6 ± 0.7
19-Pyba	45.1 ± 0.6	36.6 ± 0.4	36.1 ± 0.4	32.8 ± 0.9
19-d-Pyba	41.4 ± 0.4	35.0 ± 0.4	34.9 ± 0.5	31.2 ± 0.6
19-Per	44.7 ± 0.2	37.1 ± 0.3	37.7 ± 0.2	32.2 ± 0.6

[a] Conditions: 3.5 μM concentration of each strand, 10 mM sodium phosphate buffer, pH 7.0, 1 M NaCl.

Table 4. Thermodynamic Parameters for Duplex Association at 37 °C, as Determined from Melting Curve Data Using Meltwin at 37 °C[a]

duplex	ΔH^0 (kcal/mol)	ΔS^0 (cal/mol K)	ΔG^0 (kcal/mol)
$(TGCGCA)_2$	−38	−99	−7.1
$(TTGCGCAA)_2$	−50	−133	−8.6
(**14-Pyba**)$_2$	−51	−131	−10.9
(**14-Per**)$_2$	−48	−118	−11.0

[a] Based on the data acquired for a 4 μM strand concentration, 10 mM sodium phosphate buffer, pH 7, 1 M NaCl.

of each other, namely, **tBupyba**, **Tmsba**, **Pyba**, and **Per**. The trimethoxystilbene cap Tmsba gave the largest ΔT_m for a single mismatch (15.2 °C for A facing C), but the A:G mismatch was poorly discriminated against. The remaining three caps gave very similar melting-point depressions for mismatched duplexes, with a ΔT_m of between 12.5 (A:C) and 7.0 °C (A:G). This data confirmed that 2′-appended aromatic hydrocarbons of four (**tBupyba**, **Pyba**) or five rings (**Per**) can not only massively increase the melting point of duplexes but also improve mismatch discrimination. To shed additional light on the duplex-stabilizing effect of the optimized cap structures, we determined the enthalpy and entropy of duplex formation. For this, the self-complementary sequences were chosen, as the effect of the caps is encountered twice in their duplex form. Either of the two "winner caps", **Pyba** and **Per**, induce their duplex-stabilizing effect through a stronger enthalpic contribution to the free energy of duplex formation (Table 4). In both cases, a large portion of the enthalpic gain is lost through entropy−enthalpy compensation. The effect of either cap is much stronger than that of an additional A:T base pair, as shown by the thermodynamics of duplex formation for control compound TTGCGCAA (Table 4), whose melting point is 44.1 °C.

Discussion

These results may be discussed from several points of view. First, it is interesting to ask whether the combinatorial approach was successful. Compared to earlier studies in our and other laboratories,[39,48] the current study employed libraries of oligonucleotides with the same cap, but different linker lengths. This facilitated library generation via mixed couplings, as it required only one reactivity-adjusted mixture, namely, that of the linker building blocks. But, the use of "linker libraries" introduced more diversity on the level of the connector moiety and allowed for less diversity on the level of the caps for a given number of compounds prepared. We felt this approach was justified, as it is more difficult to design linkers that fit well than it is to design stacking moieties. Without a sufficient number of linker libraries, it would have been difficult to discern that there is indeed a clear trend toward butyric acid linkers. So, while certainly not perfect, we feel that the combinatorial approach, combined with nuclease selection from libraries of crudes, can provide answers that are difficult to obtain with the traditional approach of single compound synthesis, purification, and individual testing at the same level of effort.

There are also questions that come to mind, if one looks at the structural lessons learned. Why, for example, was a linker with four single bonds between the amide function at the 2′-position of the adenosine residue and the ring system of the cap selected as the best connector for most of the stacking moieties tested? This length (and flexibility) of such a linker is between that of the deoxyribose phosphate backbone of DNA connecting two neighboring nucleobases that stack on each other in a Watson−Crick helix and that of an ethylene bridge between two benzene rings in a paracyclophane (Figure 8). The latter presumably constitutes the shortest possible linker between two stacking aromatic rings, whereas the former allows not only for intercalation

between the nucleobases but also for unwinding and other functions enabled when nature evolved the structure of DNA. We note that the phenyl rings of paracyclophane are distorted and that linkers with three methylene units, such as those of [3.3]paracyclophane, are required for a stacking arrangement without significant strain. Presumably, our selections did not lead to the shortest possible linker, either because it does not allow for the best stacking arrangement between the aromatic rings or because the subtle interplay of other forces, including solvation, does not make such an arrangement more favorable. As a consequence, a large portion of the ~10 kcal/mol in ΔH for duplex formation that were realized with the appended pyrene or perylene ring is lost toward the entropic penalty for the formation of capped duplexes. It is worthwhile to mention that stilbene bridges optimized for bridging hairpin DNA motifs[22c] contain linker lengths very similar to the one identified in our current study but are also flexible enough to readily deviate from the arrangement that gives the most intimate stacking contact with the terminus of the DNA.[2]

Our own modeling had suggested that a direct amide link between the 2′-position of a 3′-terminal deoxynucleoside and an aromatic ring system, such as an anthracene residue, would induce stacking between nucleobase and cap, if one allows the amide linkage to rotate out of coplanarity with the anthracene rings.[49] A single methylene group as linker between the amino group of 2′-amino-LNA nucleotides and aromatic hydrocarbons is believed to disfavor stacking between the hydrocarbons and the nucleobases, however, resulting in stacks of the aromatic hydrocarbons in the minor groove.[19c] So, if more favorable, shorter linkers exist, their length will probably be between the butyric acid linker favored in our current study and a single methylene group. Whether such optimized linkers do, in fact, exist is unclear. Given that it took quite some time (and effort) to identify DNA/RNA analogs with shortened backbone that form very stable double helices in aqueous solution,[50] it might not be trivial to find them.

Second, one might ask if the diversity of stacking moieties was sufficient. In our current study, we did not employ derivatives of cationic ring systems known to intercalate into double-stranded DNA.[25] The rationale behind this was that they would have too high a propensity to intercalate and bind away from the terminal base pair we wished to stabilize. Further, it seemed likely that shape complementarity and possibly hydrogen bonding would lead to complexes with enhanced sequence selectivity, not electrostatic attraction between cationic groups and the phosphodiester backbone, whose structure is largely independent of sequence. Further, the density of anionic groups is higher in the interior of a duplex than at the termini, again making it more likely that a cationic ligand would not act as a cap, but as an intercalator. It would be interesting to complement the current collection of cap building blocks, which is rich in aromatic compounds, with more building blocks that have complex three-dimensional structures. Both the steroids tested (cholic acid and cholesterol) and the quinolones with nonplanar appendages (levofloxacin and the **Aci** cap of **17**) gave activities not much lower than that of the aromatic winner compounds.

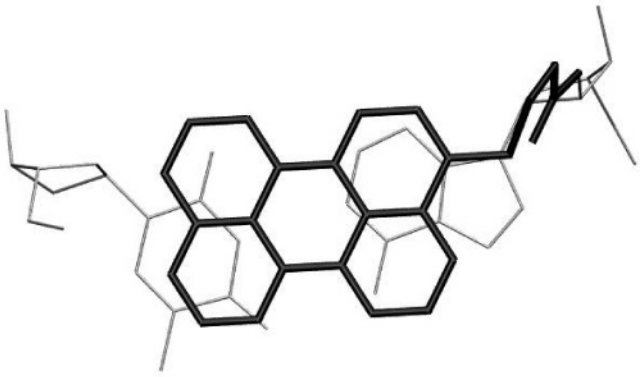

Figure 9. Overlay of an T:A Watson−Crick base pair (thin, gray lines; background) and a perylene butyramide residue (thicker, bold lines; foreground) 2′-appended to the deoxyadenine residue of the base pair. The coordinates were generated via molecular modeling in Macromodel[54] (maestro-v7.5.106), and the graphic was produced in VMD.[55]

To synthesize carboxylic acids that have the potential to engulf the entire terminus the way a folded structure of a protein can[51] remains synthetically challenging, though. Additional diversity could have been introduced, at the cost of a substantially higher synthetic effort.

Finally, one might ask why the size optimum for a cap binding to the terminus of a DNA duplex was identified as being a pyrene/perylene and how such a flat aromatic ring system increases base pairing fidelity. The observation that coronene, when identically linked to the duplex as pyrene or perylene, gives broader melting transitions and anecdotal evidence from our laboratories gained through NMR studies on DNA with large aromatic ring systems suggests that too large a stacking moiety tends to lead to aggregation and other states competing with a well-solvated, individual helix. The cap providing the largest increase in thermal stability for the duplex of TGCGCA, perylene, an aromatic hydrocarbon with five fused benzene rings, is large enough to cover a base pair (Figure 9) but is not much larger, probably avoiding the fact that too much sticky surface remains exposed upon duplex formation.

Since neither pyrene nor perylene contains hydrogen-bonding donor or acceptor functionalities, they cannot engage in H-bonds that specifically recognize an A:T base pair. So, the observation that they stabilize a duplex with an A:T base pair to a greater extent than they stabilize alternative, non-Watson−Crick base pairs must be caused by the pairing preferences of the DNA itself that are enhanced in the presence of a large lipophilic surface. Apparently, the shape of duplexes with alternative base pairs is not compatible with the binding of the aromatic caps to the same extent as that of the canonical base pair and/or the strengthening of hydrogen bonds in a more lipophilic environment provides greater selectivity. The unusually small decrease in duplex stability seen for the duplex with a terminal A:G mismatch in the presence of the **Tmsba** cap (Table 3) suggests that this is not a general phenomenon, and that the fidelity-inducing effects of aromatic appendages do depend on the structure of the cap.

Conclusions

Here we present the synthesis of a 5′-phosphoramidite building block of 2′-amino-2′-deoxyadenosine, its incorporation into oligonucleotides, and the elaboration of 2′-acylamido derivatives via mixed couplings or as individual compounds. Nuclease selection identified the residue of perylene butyric acid as the acylamido group providing the greatest increase in melting point for the hexamer 5′-TGCGCA-3′. This residue, as well as the residues of pyrene butyric acid, *tert*-butylpyrenebutyric acid, and trimethoxystilbene butyric acid was shown to induce greater base-pairing fidelity for the adenosine residue they were linked to in the non-self-complementary octamer 5′-TGGTTGAA-3′. On the basis of the very substantial enthalpy−entropy compensation determined for the formation of the perylene- and pyrene-capped duplexes, it is reasonable to propose that further improved molecular caps may be developed that feature more rigid linkers. The affinity- and fidelity-enhancing substituents presented here may find applications as modulators of target affinity for oligonucleotide probes of high-fidelity microarrays.

Experimental Section

General. DNA sequences are given from 5′- to 3′-terminus. Reagents and building blocks were from Acros (Geel, Belgium) or Aldrich/Fluka/Sigma (Deisenhofen, Germany) including adenine-9-β-D-arabinofuranoside and allyl-(1-benzotriazolyl)-carbonate (Alloc-OBt). Anhydrous solvents were purchased over molecular sieves and were used without further purification. Unmodified oligonucleotides (TGCGCA (control), **18**, **22**−**23**) were purchased from Biomers (Ulm, Germany) or Operon Biotechnologies (Cologne, Germany). The 5′-phosphoramidites of unmodified nucleosides (dA^{bz}, dC^{bz}, dG^{ibu}, dT) were obtained from ChemGenes (Wilmington, MA), and all other reagents for DNA synthesis were from Proligo (Hamburg, Germany). MALDI-TOF mass spectra were acquired on a Bruker Daltonics REFLEX IV spectrometer in negative mode using linear flight path (synthetic samples) or the reflectron (nuclease selection). The matrix mixture was made up from 2,4,6-trihydroxyacetophenone (THAP, 0.3 M in ethanol) and diammonium citrate (0.1 M in water) (2:1, v/v). Calculated masses are average masses; the *m*/*z* values found are those for pseudomolecular ions ($[M - H]^-$ or $[M + H]^+$) detected at the peak maximum. Analytical thin layer chromatography was performed on silica gel 60 precoated plates from Merck (0.25 mm thickness). Flash chromatography employed silica gel (0.063 mm-0.2 mm mesh) from Merck (Darmstadt, Germany).

2′-Azido-*N*6-benzoyl-2′-deoxy-5′,3′-*O*-(1,1,3,3-tetraisopropyldisiloxane-1,3-diyl)adenosine (4). Benzoyl chloride (758 μL, 6.54 mmol, 2 equiv) was added dropwise to a solution of **3** (1.748 g, 3.27 mmol) in anhydrous pyridine (9.5 mL) at 0 °C. After 5 min, the yellow solution was allowed to thaw and was stirred at room temp for 2.5 h. Then, the solution was cooled to 0 °C, and morpholine (1.14 mL, 13.1 mmol, 4 equiv) was added. After 45 min at 0 °C, CH_2Cl_2 (190 mL) was added, followed by the addition of water (190 mL) and isolation of the organic phase. The organic phase was dried over $MgSO_4$ and the solvent was evaporated in vacuo. The residue was purified by column chromatography (silica, hexanes/ethyl acetate, 1:1), yielding 2.05 g of **4** (3.2 mmol, 98%). TLC (hexanes/ethyl acetate, 1:1): $R_f = 0.26$. ^{1}H NMR (500 MHz, $CDCl_3$): δ 9.18 (bs, 1H, N−*H*), 8.79 (s, 1H, *H8*), 8.23 (s, 1H, *H2*), 8.05 (d, J = 7.2 Hz, 2H, Ar−H_{ortho}), 7.63 (dd, J = 7.2 Hz, J = 7.9 Hz, 1H, Ar−H_{para}), 7.54 (dd, J = 7.9 Hz, J = 7.2 Hz, 2H, Ar−H_{meta}), 5.86 (s, 1H, *H1′*), 5.21 (dd, J = 9.1 Hz, J = 5.7 Hz, 1 H, *H3′*), 4.66 (d, J = 5.7 Hz, 1 H, *H2′*), 4.16 (d, J = 9.1 Hz, 1H, *H4′*), 4.21 (dd, J = 13.9, J = 2.8, 1H, *H5′*), 4.07 (dd, J = 13.91 Hz, J = 2.8 Hz, 1H, *H5″*), 1.14 − 1.08 (m, 28 H, *TIPS*). ^{13}C NMR (126 MHz, $CDCl_3$): δ 164.7, 152.7, 150.8, 149.7, 141.6, 133.6, 132.9, 128.9, 127.9, 123.6, 87.4, 81.9, 71.0, 65.3, 59.9, 17.4, 17.4, 17.4, 17.3, 17.2, 17.0, 17.0, 16.9, 13.4, 13.0, 12.7, 12.7. MS (FAB): 639.4 $(M + H)^+$.

2′-Amino-*N*6-benzoyl-2′-deoxy-5′,3′-*O*-(1,1,3,3-tetraisopropyldisiloxane-1,3-diyl)adenosine (5). Methanol (25 mL) was added to a mixture of **4** (2.80 g, 4.57 mmol) and Pd/C (280 mg), and the resulting slurry was stirred for 14 h under a H_2 atmosphere, until TLC showed full conversion of the starting material. The catalyst was filtered off over kieselgur, and the filter cake was washed several times with hot methanol. The methanolic solutions were combined, and the solvent was evaporated in vacuo. The residue was purified by column chromatography (silica, CH_2Cl_2/MeOH/NEt_3, 90:10:1) to give the title compound, **5**, (2.627 g, 4.286 mmol, 94%). TLC (CH_2Cl_2/MeOH/NEt_3, 90:10:1): $R_f = 0.52$. ^{1}H NMR (500 MHz, $CDCl_3$): δ 9.23 (bs, 1H, N−*H*), 8.77 (s, 1H, *H8*), 8.29 (s, 1H, *H2*), 8.02 (d, J = 7.5 Hz, 2H, Ar−H_{ortho}), 7.60 (d, J = 7.5 Hz, 1H, Ar−H_{para}), 7.51 (dd, J = 7.53 Hz, J = 7.54 Hz, 2H, Ar−H_{meta}), 6.00 (d, J = 1.9 Hz, 1H, *H1′*), 4.78 (dd, J = 7.2 Hz, J = 6.9 Hz, 1H, *H3′*), 4.26 (m, 1H, *H4′*), 4.16 (dd, J = 4.1 Hz, J = 12.9 Hz, 1 H, *H5′*), 4.07 (dd, J = 4.1 Hz, J = 12.9 Hz, 1H, *H5″*), 3.99 (dd, J = 1.9 Hz, J = 6.6 Hz, 1H, *H2′*), 2.26 (bs, 2H, NH_2), 1.12−1.02 (m, 28H, TIPS). ^{13}C NMR (126 MHz, $CDCl_3$): δ 164.7, 152.6, 151.2, 149.5, 141.6, 133.7, 132.8, 128.8, 127.9, 123.6, 90.3, 82.9, 69.9, 61.5, 58.1, 17.5, 17.4, 17.3, 17.2, 17.1, 17.0, 17.0, 13.4, 13.1, 13.0, 12.6. MS (FAB): 613.3 $(M + H)^+$.

***N*2′-Allyloxycarbonyl-2′-amino-*N*6-benzoyl-2′-deoxy-5′,3′-*O*-(1,1,3,3-tetraisopropyldisiloxane-1,3-diyl)adenosine (6).** A mixture of **5** (404 mg, 0.659 mmol) and allyloxycarbonyloxybenzotriazol (173 mg, 0.791 mmol, 1.2 equiv) was dissolved in anhydrous pyridine (6.6 mL). After the mixture was stirred at room temp for 3 h, the solution was diluted with CH_2Cl_2 (30 mL) and washed with aqueous citric acid solution (5% m/v, 30 mL) and saturated $NaHCO_3$ solution (30 mL). The solvent was evaporated, and the resulting yellow oil was purified by column chromatography (silica, hexanes/ethyl acetate, 1:1) to give 330 mg of **6** (0.474 mmol, 72%). TLC (hexanes/ethyl acetate 1:1): $R_f = 0.18$. ^{1}H NMR (500 MHz, $CDCl_3$): δ 9.20 (bs, 1H, N−*H*), 8.77 (s, 1H, *H8*), 8.21 (s, 1H, *H2*), 8.04 (d, J = 7.9 Hz, 2H, Ar−H_{ortho}), 7.62 (d, J = 7.5 Hz, 1H, Ar−H_{para}), 7.54 (dd, J = 7.5 Hz, J = 7.9 Hz, 2H, Ar−H_{meta}), 6.10 (bs, 1H, *H1′*), 5.86−5.96 (m, 1H, Alloc-CH_2−C*H*−CH_2), 5.73 (bs, 1H, *H3′*), 5.33 (bs, 1H, *H4′*), 5.24−5.30 (m, 2H, Alloc-CH_2−CH−*CH_2*), 4.65 (m, 1H, *H2′*), 4.57 (m, 2H, Alloc-*CH_2*−CH−CH_2), 4.08

(bs, 2H, *H5′ H5″*), 1.19−1.08 (m, 28H, TIPS). ^{13}C NMR (126 MHz, $CDCl_3$): δ 164.6, 156.5, 152.5, 151.4, 149.7, 142.6, 133.7, 132.8, 132.3, 128.9, 127.9, 123.4, 118.3, 88.5, 83.7, 70.0, 66.2, 62.3, 57.0, 17.5, 17.4, 17.3, 17.3, 17.1, 17.0, 17.0, 16.9, 13.2, 13.1, 12.9, 12.5. MS (FAB): 697.3 $(M + H)^+$.

***N2′*Allyloxycarbonyl-2′-amino-*N6*-benzoyl-2′-deoxyadenosine (7)**. Compound **6** (1.57 g, 2.26 mmol) was dissolved in anhydrous THF (5 mL). Then, TBAF (1 M in THF, 5.3 mL, 5.3 mmol, 2.1 equiv) was added. After the mixture was stirred for 45 min at room temp, TLC showed full conversion. $MeOSiMe_3$ (1.4 mL, 10.1 mmol, 4 equiv) was added, and after it was stirred an additional 15 min, the reaction solution was directly applied to a silica column and eluted with CH_2Cl_2/MeOH (9:1). The product-containing fractions gave 938 mg of **7** (2.06 mmol, 91%). TLC (CH_2Cl_2/MeOH 9:1): $R_f = 0.42$. ^{1}H NMR (500 MHz, DMSO-d_6): δ 11.25 (s, 1H, N*H*−Bz), 8.78 (s, 1H, *H8*), 8.67 (s, 1H, *H2*), 8.06 (d, $J = 7.5$ Hz, 2H, Ar−H_{ortho}), 7.66 (dd, $J = 7.2$ Hz, $J = 7.5$, 1H, Ar−H_{para}), 7.57 (dd, $J = 7.2$ Hz, $J = 7.5$ Hz, 2H, Ar−H_{meta}), 7.42 (d, $J = 8.5$ Hz, 1H, N*H*−Alloc), 6.14 (d, $J = 8.16$ Hz, 1H, *H1′*), 5.87−5.78 (m, 1H, Alloc-CH_2−C*H*−CH_2), 5.79 (bs, 1H, 3′-O*H*), 5.23 (d, $J = 17.0$ Hz, 1H, Alloc-CH_2−CH−CH_2), 5.12 (d, $J = 10.4$ Hz, 1H, Alloc-CH_2−CH−CH_2), 4.97 (m, $J = 8.2$ Hz, 1H, *H2′*), 4.34−4.44 (m, 2H, Alloc-CH_2-CH−CH_2), 4.29 (s, 1H, *H3′*), 4.07 (s, 1H, *H4′*), 3.72 (m, 1H, *H5′*), 3.62 (m, 1H, *H5″*). ^{13}C NMR (126 MHz, DMSO-d_6): δ 166.1, 156.2, 152.8, 152.2, 151.0, 143.8, 133.7, 133.7, 133.0, 129.0, 126.4, 117.7, 87.7, 86.2, 70.6, 65.2, 62.2, 57.2, 55.4. MS (FAB): 455.2 $(M + H)^+$.

***N2′*-Allyloxycarbonyl-2′-amino-*N6*-benzoyl-2′-deoxy-5′-*O*-dimethoxytrityladenosine (8).** A mixture of **7** (1.20 g, 2.64 mmol), DMT-Cl (1.074 g, 3.17 mmol, 1.2 equiv), and DMAP (30 mg) was dissolved in anhydrous pyridine (13 mL), followed by stirring at room temp for 2 h. Then, MeOH (10 mL) was added. After the mixture was stirred for 1 h, the solvents were evaporated, and the residue was taken up in CH_2Cl_2 (200 mL) and washed with aqueous citric acid solution (200 mL, 5% m/v) and saturated $NaHCO_3$ solution (200 mL). The organic phase was dried over Na_2SO_4, and the solvent was evaporated in vacuo. The residue was purified by column chromatography (silica, ethyl acetate, 1% NEt_3), yielding 1.70 g of **8** (2.24 mmol, 85%). TLC (ethyl acetate, 1% NEt_3): $R_f = 0.36$. ^{1}H NMR (400 MHz, $CDCl_3$): δ 9.10 (s, 1H, N*H*-Bz), 8.63 (s, 1H, *H8*), 8.27 (s, 1H, *H2*), 7.90 (d, $J = 7.3$ Hz, 2H, Bz-H_{ortho}), 7.51 (d, $J = 7.6$ Hz, 1H, Bz-H_{para}), 7.41 (dd, $J = 7.6$ Hz, $J = 7.3$ Hz, 2H, Alloc-CH_2−CH−CH_2), 4.97 (m, 1H, *H2′*), 4.59 (d, $J = 4.0$ Hz, 1H, *H3′*), 4.31 (m, 2H, Alloc-CH_2−CH−CH_2), 4.26 (s, 1H, *H4′*), 3.67 (s, 6H, DMT−OMe), 3.40−3.29 (m, 2H, *H5′ H5″*). ^{13}C NMR (100 MHz, $CDCl_3$): δ 164.8, 158.6, 156.1, 152.6, 152.2, 149.4, 144.4, 142.0, 135.5, 133.6, 132.9, 132.3, 130.1, 128.9, 128.2, 128.0, 127.9, 127.0, 123.0, 118.0, 113.3, 86.8, 86.3, 85.6, 71.7, 66.0, 63.7, 57.7, 55.2. MS (FAB): 757.3 $(M + H)^+$.

***N2′*,*O3′*-Bis[allyloxycarbonyl]-2′-amino-*N*6-benzoyl-2′-deoxy-5′-*O*-dimethoxytrityladenosine (9).** A mixture of **8** (1.68 g, 2.22 mmol), *N*1-(allyloxycarbonyloxy)-7-azabenzotriazole[54] (587 mg, 2.67 mmol, 1.2 equiv), and DMAP (27 mg, 0.22 mmol, 0.1 equiv) was dissolved in anhydrous pyridine (22 mL). After the mixture was stirred for 5.5 h at room temp, another portion of allyloxycarbonyloxyazabenzotriazole (325 mg, 1.48 mmol, 0.66 equiv) was added. After the mixture was stirred for another 23 h at room temp, a third portion of allyloxycarbonyloxyazabenzotriazole (120 mg, 0.545 mmol, 0.26 equiv) was added. After 28 h, TLC showed full conversion. Methanol (5 mL) was added, followed by evaporation of the solvents in vacuo. The residue was taken up in CH_2Cl_2 (200 mL) and washed with aqueous citric acid solution (150 mL, 5% m/v) and saturated aqueous $NaHCO_3$ (150 mL). The organic layer was dried over Na_2SO_4, and the solvent was evaporated in vacuo. The residue was purified by column chromatography (silica, hexanes/ethyl acetate/NEt_3, 1:2:0.06) to give 1.34 g (1.59 mmol, 72%) of **9**. TLC (hexanes/ethyl acetate/NEt_3, 1:2:0.06): $R_f = 0.36$. ^{1}H NMR (500 MHz, $CDCl_3$): δ 9.11 (s, 1H, N*H*-Bz), 8.77 (s, 1H, *H8*), 8.34 (s, 1H, *H2*), 8.03 (d, $J = 7.5$ Hz, 2H, Bz-H_{ortho}), 7.61 (d, $J = 7.5$ Hz, 1H, Bz-H_{para}), 7.52 (dd, $J = 7.5$ Hz, $J = 8.2$ Hz, 2H, Bz-H_{meta}), 7.47 (d, $J = 7.85$ Hz, 2H, DMT Ph H_{meta}), 7.36 (d, $J = 9.1$ Hz, 4H, DMT MeOPh H_{meta}), 7.29−7.34 (m, 2H, DMT Ph H_{ortho}), 7.25 (dd, $J = 7.9$ Hz, $J = 7.2$ Hz, 1H, DMT Ph H_{para}), 6.85 (dd, $J = 8.5$ Hz, $J = 3.5$ Hz, 4 H, DMT MeOPh H_{ortho}), 6.30 (d, $J = 7.5$ Hz, 1H, *H1′*), 5.99−5.91 (m, 1H, Alloc-CH_2−C*H*−CH_2), 5.87−5.79 (m, 1H, Alloc-CH_2−C*H*−CH_2), 5.53−5.49 (m, 1H, *H2′*), 5.39−5.38 (m, 1H, *H3′*), 5.44−5.33 (m, 2H, Alloc-CH_2−CH−CH_2), 5.28−5.16 (m, 2H, Alloc-CH_2−CH−CH_2), 4.70−4.66 (m, 2H, Alloc-CH_2-CH−CH_2), 4.56−4.43 (m, 2H, Alloc-CH_2-CH−CH_2), 4.42 (bs, 1H, *H4′*), 3.80 (d, $J = 1.9$ Hz, 6H, DMT-OCH_3), 3.56−3.53 (m, 2H, *H5′*, *H5″*). ^{13}C NMR (126 MHz, $CDCl_3$): δ 164.6, 158.7, 155.4, 153.8, 152.9, 152.5, 149.6, 144.2, 141.2, 135.3, 133.7, 132.8, 132.1, 130.8, 130.1, 130.1, 128.9, 128.1, 128.1, 127.9, 127.1, 123.2, 119.9, 118.4, 113.4, 87.2, 85.1, 83.6, 69.3, 66.3, 63.5, 56.0, 55.3. MS (FAB): 841.2 $(M + H)^+$.

***N2′*,*O3′*-Bis[allyloxycarbonyl]-2′-amino-*N*6-benzoyl-2′-deoxyadenosine (10).** Compound **9** (1.09 g, 1.29 mmol) was dissolved in CH_2Cl_2 (13 mL). Then, TFA (80% in water, 660 μL, 4.63 mmol, 3.6 equiv) was added. After the mixture was stirred for 40 min at room temp, the red suspension was diluted with CH_2Cl_2 (100 mL) and washed twice with water (100 mL) and with a saturated $NaHCO_3$ solution (100 mL). The organic layer was dried over Na_2SO_4, and the solvent was evaporated in vacuo. The resulting orange foam was purified by column chromatography (silica, ethyl acetate) yielding 624 mg (1.161 mmol, 90%) of **10**. TLC (ethyl acetate): $R_f = 0.66$. ^{1}H NMR (500 MHz, $CDCl_3$): δ 9.25 (s, 1H, N*H*Bz), 8.79 (s, 1H, *H8*), 8.12 (s, 1H, *H2*), 8.02 (d, $J = 7.5$ Hz, 2H, Bz-H_{ortho}), 7.61 (m, 1H, Bz-H_{para}), 7.52 (dd, $J = 7.23$ Hz, $J = 7.5$ Hz, 2H, Bz-H_{meta}), 6.10 (d, $J = 10.7$ Hz, 1H, 5′-O*H*), 5.96 (m, 1H, *H1′*), 6.00−5.90 (m, 1H, Alloc-CH_2−C*H*−CH_2), 5.84−5.73 (m, 1H, Alloc-CH_2−C*H*−CH_2), 5.50−5.44 (m, 1H, *H2′*), 5.25−5.13 (m, 2H, Alloc-CH_2−CH−CH_2), 5.61 (d, $J = 8.5$ Hz, 1H, *H3′*), 5.44−5.33 (m, 2H, Alloc-CH_2−CH−CH_2), 4.73−4.65 (bs, 2H, Alloc-CH_2−CH−CH_2), 4.40 (bs, 3H, Alloc-CH_2−CH−CH_2, *H4′*), 4.05−3.90 (m, 2H, *H5′*, *H5″*). ^{13}C NMR (126 MHz, $CDCl_3$): δ 164.7, 155.2, 153.7, 152.3, 151.0, 150.3, 142.6, 133.5, 132.9,

132.1, 130.8, 128.9, 128.0, 124.6, 120.2, 118.5, 89.8, 86.4, 78.1, 69.4, 66.3, 62.9, 55.2. MS (FAB): 539.1 $(M + H)^+$.

***N*2′,*O*3′-Bis[allyloxycarbonyl]-2′-amino-*N*6-benzoyl-2′-deoxyadenosine-5′-*O*-yl-cyanoethyl-*N*,*N*-diisopropylphosphoramidite (1)**. Compound **10** (556 mg, 1.034 mmol) was dissolved in anhydrous acetonitrile (10 mL), and a few beads of molecular sieves (3 Å) were added. After the mixture was stirred for 20 min at room temp under Ar, diisopropylethylamine (513 μL, 3.103 mmol, 3 equiv) and then 2-cyanoethyl-*N*,*N*-diisopropylchlorophosphoramidite (489 mg, 2.069 mmol, 2 equiv) were added. After 0.5 h, TLC showed full conversion of **10**. The solution was diluted with CH_2Cl_2 (100 mL) and washed with a saturated aqueous $NaHCO_3$ solution (100 mL). The organic layer was dried over Na_2SO_4, and the solvent was evaporated in vacuo. The residue was purified by rapid column chromatography (silica, ethyl acetate/NEt_3, 98:2) yielding 644 mg (0.873 mmol, 84%) of the title compound as a mixture of diastereomers. TLC (ethyl acetate/NEt_3, 98:2): $R_f = 0.78$. ^{31}P NMR (101 MHz, CD_3CN): δ 150.3, 150.2. MALDI-TOF MS: *m*/*z* 739.0 $[M + H]^+$.

DNA Synthesis. The unmodified portion of oligodeoxynucleotides was prepared on a 1 μmol scale using a Perseptive Biosystems 8909 Expedite DNA synthesizer and the protocol provided by the manufacturer. Reaction columns for DNA synthesis were from Prime Synthesis (Aston, PA). The couplings of nonstandard phosphoramidite (**1**) to solid support-bound DNA used a 0.1 M solution (300 μL) of the phosphoramidite in MeCN, the same volume of activator solution (1*H*-tetrazole, 0.4 M in CH_3CN), and a reaction time of 60 min, followed by standard oxidation and deprotection steps.

HPLC Purification. Oligonucleotides were HPLC purified on a Merck-Hitachi L-6200 system with a photodiodarray detector on a 250 mm × 4.6 mm Nucleosil C4 column (Macherey-Nagel, Düren, Germany), using a gradient of CH_3CN (solvent B) in 0.1 M triethylammonium acetate, pH 7, with detection at 260 nm. Yields of oligonucleotides are based on the intensity of the product peak in the HPLC trace of the crude.

Coupling of Phosphoramidite Building Block 1 to Support 11 and Removal of Alloc Groups. A sample of cpg-bound DNA (**11**, 20 mg, 1 μmol loading) was added to 2′-amino-2′-deoxyadenosine phosphoramidite **1** (50 μmol, 36.9 mg, 50 equiv) and dried at 0.1 Torr for 30 min. Then, anhydrous MeCN (250 μL) and a 4,5-dicyanoimidazole activator solution (0.25 M in MeCN, 250 μL) was added. The resulting slurry was vortexed for 1 h at room temp. Then, the supernatant was aspirated, and the support was washed three times with acetonitrile (800 μL each). Then, the oxidizer solution for DNA synthesis (iodine 1 M in pyridine/THF/water, 21:77:2 v/v, 800 μL) was added. After the mixture was vortexed for 20 min, the solid support was washed several times with DMF and then MeCN (800 μL each) until it was colorless. After the support was dried at 0.1 Torr for 30 min, triphenyl phosphine (0.75 mg, 2.86 μmol), tetrakis-[triphenylphosphine]palladium (3.75 mg, 3.25 μmol), and $[Et_2NH_2]^+[HCO_3]^-$ (3.75 mg, 27.74 μmol) in anhydrous CH_2Cl_2 (500 μL) were added, followed by vortexing. After the mixture was vortexed for 2.5 h, the supernatant was aspirated, and the support was washed several times with CH_2Cl_2, then DMF containing 1% NEt_3, and neat DMF (800 μL each), followed by drying at 0.1 Torr.

Mixed Coupling with Linker Amino Acid Building Blocks. Stock solutions (0.5 M in DMF) Fmoc-Gly-OH (172 mg, 1000 μmol in 2 mL DMF), Fmoc-β-Ala-OH (198 mg, 636 μmol in 1,27 mL DMF), Fmoc-γ-amino butyric acid (155 mg, 476 μmol in 953 μL DMF), Fmoc-Pro-OH (204 mg, 605 μmol in 1.21 mL DMF), and Fmoc-ϵ-amino hexanoic acid (212 mg, 600 μmol in 1.20 mL DMF) were prepared. Separate stock solutions of HATU and HOAt (0.475 M each, in DMF) were generated. Individual activation of the amino acid building block in separate vessels were induced by combination of aliquots for the conversion of Fmoc-Gly-OH (120 μL amino acid stock solution, 60 μL HOAt stock solution, 60 μL HATU stock solution, 23 μL DIEA), Fmoc-β-Ala-OH (30 μL amino acid stock solution, 15 μL HOAt stock solution, 15 μL HATU stock solution, 5.8 μL DIEA), Fmoc-γ-amino butyric acid (40 μL amino acid stock solution, 20 μL HOAt stock solution, 20 μL HATU stock solution, 7.6 μL DIEA), Fmoc-Pro-OH (40 μL amino acid stock solution, 20 μL HOAt stock solution, 20 μL HATU stock solution, 7.6 μL DIEA), and Fmoc-ϵ-amino hexanoic acid (40 μL amino acid stock solution, 20 μL HOAt stock solution, 20 μL HATU stock solution, 7.6 μL DIEA). After 15 min at room temp, the activation solutions were pooled into one vessel and mixed, and the resulting solution was added to the solid support-bound DNA (3 mg, ∼0.15 μmol loading). The coupling reaction was allowed to proceed at 50 °C (water bath) for 40 min. The supernatant was aspirateded, and the support was washed several times with DMF and MeCN (800 μL each) and dried at 0.1 Torr for 30 min.

Coupling of Carboxylic Acid Caps to Solid Support-Bound Oligonucleotides. The procedure for coupling the carboxylic acids featuring the stacking moieties was similar to that for the mixture of linker amino acids. Briefly, a mixture of the carboxylic acid in question (100 μmol), HATU (36 mg), and diisopropylethylamine (38 μL) was dissolved in anhydrous DMF (400 μL). After 15 min at room temp, the solution was added to the solid support-bound DNA (3 mg, ∼0.15 μmol loading) in a polypropylene cup, followed by vortexing. The vessel was placed in a waterbath at 50 °C for 45 min with occasional vortexing. Then, the support was washed several times with DMF and MeCN.

Deprotection and Release from Solid Support. A sample of the fully assembled oligonucleotide hybrid (typically 3 mg, ∼0.15 μmol loading) was placed in a polypropylene cup and was treated with saturated aqueous ammonia (0.5 mL) for 14 h at room temperature. Then, the excess ammonia was removed by directing a gentle flow of compressed air onto the surface of the solution for 20 min. Then, the supernatant was aspirated, and the support was washed twice with water (0.2 mL) containing aqueous ammonia (20 μL). The combined aqueous solutions were lyophilized to dryness, taken up in water, and the resulting stock solution was either used for selection assays or subjected to HPLC purification.

Nuclease Selection. A solution of the oligonucleotide mixture (1.5 nmol total) in water (1.5 μL) was mixed with ammonium acetate buffer (0.5 M NH_4OAc in H_2O, 6 μL, pH 7.0) in a polypropylene vessel cup (void volume 0.5 mL). Then, a solution of bovine spleen phosphodiesterase II (E.C. 3.1.16.1) with an activity of 0.05 u/μL in aqueous NH_4OAc buffer (0.5 M, 1.5 μL, pH 7.0) was added, followed by vortexing and centrifugation, and the reaction vessel was placed in a water bath at 25 °C. Samples (0.5 μL) were drawn immediately after mixing, as well as 5, 15, 30, 60, 90, 120, 180, 240, and 300 min after initiation of the nuclease assay. Each solution drawn was added to a MALDI matrix mixture, made up of a solution of trihydroxyacetophenone in EtOH/diammonium citrate in water (4:1; 3 μL total) that contained 20 pmol of DNA oligomer 5′-CATTGACA-3′ as internal standard, as well as a few grains of Dowex 50WX8-200 cation-exchange resin (ammonium form). From the resulting mixture, 1 μL was spotted onto the MALDI target. Between 3 and 5 MALDI-TOF spectra were acquired per time point in negative mode of the spectrometer with the reflectron switched on. Data analysis followed the procedure described in ref 10a. Briefly, a computer program called DAS automatically integrated the peaks of the mixture components and produced relative peak intensity values to the peak of the internal standard. Protection factors were calculated from the values thus obtained using software written in-house dubbed Automaton,[55] version 2, with cutoff and truncation set to 20%. Both computer programs (DAS and Automaton) may be downloaded from the web page of the authors free of charge.

Analytical Data for Modified Oligonucleotides that Were HPLC Purified.

14-Per. Yield: 43%. HPLC: CH_3CN gradient 0−20% in 2 min, 20−40% in 28 min, t_R = 17 min. MALDI-TOF MS for $C_{82}H_{90}N_{24}O_{35}P_5$ $[M - H]^-$: calcd 2126.1, found 2126.1.

14-Cor. Yield: 50%. HPLC: CH_3CN gradient 0−20% in 2 min, 20−35% in 28 min, t_R 20 min. MALDI-TOF MS for $C_{86}H_{90}N_{24}O_{35}P_5$ $[M - H]^-$: calcd 2174.6, found 2173.5.

14-Pyba. Yield: 46%. HPLC: CH_3CN gradient gradient 0−10% in 1 min, 10−17% in 28 min, t_R = 17 min. MALDI-TOF MS for $C_{78}H_{88}N_{24}O_{35}P_5$ $[M - H]^-$: calcd 2076.5, found 2075.6.

16-e-Lev. Yield: 49%. HPLC: CH_3CN gradient gradient 0−13% in 2 min, 13−20% in 28 min, t_R = 26 min. MALDI-TOF MS for $C_{82}H_{103}FN_{28}O_{38}P_5$ $[M - H]^-$: calcd 2262.7, found 2263.8.

14-Hmaq. Yield: 27%. HPLC: CH_3CN gradient 0−15% in 2 min, 15−30% in 28 min, t_R = 13 min. MALDI-TOF MS for $C_{75}H_{84}N_{24}O_{38}P_5$ $[M - H]^-$: calcd 2084.5, found 2083.1.

14-Tmsba. Yield: 25%. HPLC: CH_3CN gradient 0−17% in 2 min, 17−35% in 28 min, t_R = 17 min. MALDI-TOF MS for $C_{79}H_{96}N_{24}O_{38}P_5$ $[M - H]^-$: calcd 2144.6, found 2143.5

14-tBupyba. Yield: 42%. HPLC: CH_3CN 0−20% in 2 min, 20−35% in 28 min, t_R = 26 min. MALDI-TOF MS for $C_{84}H_{102}N_{24}O_{35}P_5$ $[M - H]^-$: calcd 2132.7, found 2133.2.

16-b-Chol. Yield: 52%. HPLC: CH_3CN gradient 0−15% in 2 min, 15−28% in 28 min, t_R = 25 min. MALDI-TOF MS for $C_{85}H_{117}N_{25}O_{39}P_5$ $[M - H]^-$: calcd 2267.9, found 2267.7.

16-d-Chol. Yield: 47%. HPLC: CH_3CN gradient 0−20% in 2 min, 20−32% in 28 min, t_R = 20 min. MALDI-TOF MS for $C_{87}H_{119}N_{25}O_{39}P_5$ $[M - H]^-$: calcd 2293.9, found 2291.8.

16-b-Tms. Yield: 43%. HPLC: CH_3CN gradient 0−10% in 1 min, 10−35% in 29 min, t_R = 22 min. MALDI-TOF MS for $C_{79}H_{95}N_{25}O_{39}P_5$ $[M - H]^-$: calcd 2173.6, found 2171.8.

16-b-Py. Yield: 45%. HPLC: CH_3CN gradient 0−15% in 2 min, 15−20% in 28 min, t_R = 18 min. MALDI-TOF MS for $C_{78}H_{87}N_{25}O_{36}P_5$ $[M - H]^-$: calcd 2105.5, found 2105.0.

16-c-Aq. Yield: 55%. HPLC: CH_3CN gradient 0−18% in 2 min, 18−23% in 28 min, t_R = 16 min. MALDI-TOF MS for $C_{77}H_{87}N_{25}O_{38}P_5$ $[M - H]^-$: calcd 2125.5, found 2125.2.

16-c-Lev. Yield: 29%. HPLC: CH_3CN gradient 0−13% in 2 min, 13−20% in 28 min, t_R = 25 min. MALDI-TOF MS for $C_{80}H_{99}FN_{28}O_{38}P_5$ $[M - H]^-$: calcd 2234.7, found 2233.3.

14-Chol. Yield: 47%. HPLC: CH_3CN gradient 0−13% in 2 min, 13−23% in 28 min, t_R = 14 min. MALDI-TOF MS for $C_{82}H_{112}N_{24}O_{38}P_5$ $[M - H]^-$: calcd 2196.8, found 2196.0.

16-d-Aq. Yield: 34%. HPLC: CH_3CN gradient 0−27% in 10 min, 27−35% in 20 min, t_R = 22 min. MALDI-TOF MS for $C_{78}H_{87}N_{24}O_{38}P_5$ $[M - H]^-$: calcd 2137.5, found 2138.1.

14-Aq. Yield: 23%. HPLC: CH_3CN gradient 0−45% in 30 min, t_R = 21 min. MALDI-TOF MS for $C_{73}H_{80}N_{24}O_{37}P_5$ $[M - H]^-$: calcd 2040.4, found 2041.4.

16-b-Pyba. Yield: 55%. HPLC: CH_3CN gradient 0−13% in 2 min, 13−22% in 28 min, t_R = 28 min. MALDI-TOF MS for $C_{81}H_{93}N_{25}O_{36}P_5$ $[M - H]^-$: calcd 2147.6, found 2146.7.

16-d-Pyba. Yield: 58%. HPLC: CH_3CN gradient 0−45% in 30 min, t_R = 27 min. MALDI-TOF MS for $C_{83}H_{95}N_{25}O_{36}P_5$ $[M - H]^-$: calcd 2173.7, found 2173.1.

Compound 17. Yield: 10%. HPLC: CH_3CN gradient 0−5% in 1 min, 5−20% in 29 min, t_R = 20 min. MALDI-TOF MS for $C_{80}H_{94}N_{31}O_{44}P_6$ $[M - H]^-$: calcd 2379.6, found 2362.5.

16-b-Aq. Yield: 51%. HPLC: CH_3CN gradient 0−35% in 30 min, t_R = 25 min. MALDI-TOF MS for $C_{76}H_{85}N_{25}O_{38}P_5$ $[M - H]^-$: calcd 2111.5, found 2110.5.

16-c-Chr. Yield: 60%. HPLC: CH_3CN gradient 0−15% in 2 min, 15−30% in 28 min, t_R = 13 min. MALDI-TOF MS for $C_{81}H_{91}N_{25}O_{36}P_5$ $[M - H]^-$: calcd 2145.6, found 2144.8.

16-b-Chr. Yield: 52%. HPLC: CH_3CN gradient 0−15% in 2 min, 15−30% in 28 min, t_R = 12 min. MALDI-TOF MS for $C_{80}H_{89}N_{25}O_{36}P_5$ $[M - H]^-$: calcd 2131.6, found 2132.0.

16-d-Chr. Yield: 61%. HPLC: CH_3CN gradient 0−10% in 1 min, 10−40% in 29 min, t_R = 23 min. MALDI-TOF MS for $C_{82}H_{91}N_{25}O_{36}P_5$ $[M - H]^-$: calcd 2157.6, found 2150.0.

19-b-Chr. Yield: 74%. HPLC: CH_3CN gradient 0−5% in 1 min, 5−16% in 29 min. t_R = 25 min. MALDI-TOF MS for $C_{102}H_{114}N_{36}O_{47}P_7$ $[M - H]^-$: calcd 2813.0, found 2812.6.

19-Tmsba. Yield: 26%. HPLC: CH_3CN gradient 0−10% in 1 min, 10−40% in 29 min, t_R = 23 min. MALDI-TOF MS for $C_{101}H_{121}N_{35}O_{49}P_7$ $[M - H]^-$: calcd 2826.1, found 2825.7.

19-tBupyba. Yield: 41%. HPLC: CH_3CN gradient 0−20% in 2 min, 20−45% in 28 min, t_R = 22 min. MALDI-TOF MS for $C_{104}H_{121}N_{35}O_{46}P_7$ $[M - H]^-$: calcd 2814.1, found 2814.4.

19-Per. Yield: 25%. HPLC: CH_3CN gradient 0−20% in 2 min, 20−30% in 28 min, t_R = 24 min. MALDI-TOF MS for $C_{104}H_{115}N_{35}O_{46}P_7$ $[M - H]^-$: calcd 2808.1, found 2806.8.

19-c-Lev. Yield: 58%. HPLC: CH_3CN gradient 0−18% in 2 min, 18−23% in 28 min, t_R = 11 min. MALDI-TOF MS for $C_{102}H_{124}FN_{39}O_{49}P_7$ $[M - H]^-$: calcd 2916.1, found 2916.9.

19-d-Pyba. Yield: 43%. HPLC: CH_3CN gradient 0−20% in 2 min, 20−30% in 28 min, t_R = 12 min. MALDI-TOF MS for $C_{105}H_{120}N_{36}O_{47}P_7$ $[M - H]^-$: calcd 2855.1, found 2853.3.

19-b-Aq. Yield: 73%. HPLC: CH_3CN gradient 0−10% in 1 min, 10−18% in 29 min, t_R = 11 min. MALDI-TOF MS for $C_{98}H_{110}N_{36}O_{49}P_7$ $[M - H]^-$: calcd 2793.0, found 2793.4.

19-Pyba. Yield: 60%. HPLC: CH_3CN gradient 0−10% in 1 min, 10−27% in 29 min, t_R = 24 min. MALDI-TOF MS for $C_{100}H_{113}N_{35}O_{46}P_7$ $[M - H]^-$: calcd 2758.0, found 2756.2.

UV-Melting Experiments. UV-melting curves were acquired on a Perkin-Elmer Lambda 10 spectrophotometer at 260 nm with a 1 cm path length at heating or cooling rates of 1 °C/min. For the self-complementary sequence, the strand concentration was 4 μM in 10 mM sodium phosphate buffer pH 7. Melting curves were acquired without NaCl or with 150 mM and 1 M NaCl. For the melting curve study on mismatch discrimination, the DNA concentration was 3.5 μM (each strand) in a sodium phosphate buffer (10 mM) and 1 M NaCl. Melting temperatures were determined with UV Winlab 2.0 (Perkin-Elmer) and are averages of the maxima of the first derivative of the 95-point smoothed curves from heating and cooling experiments. Hyperchromicity was calculated using the difference in adsorption between the high- and low-temperature baseline and dividing by the adsorption at the low-temperature baseline.

Acknowledgment. The authors are grateful to K. Siegmund for help with computer issues and P. Grünefeld and C. Deck for a review of the manuscript. This work was supported by DFG (Grants RI 1063/4-3 and FOR 434) and the Fonds der Chemischen Industrie (Project 164431). M.P. is a recipient of a predoctoral fellowship from the State of Baden Württemberg.

Supporting Information Available. Synthetic procedures for carboxylic acid building blocks that are not commercially available, NMR spectra of new small molecules, and MALDI-TOF mass spectra of modified oligonucleotides. This material is available free of charge via the Internet at http://pubs.acs.org.

References and Notes

(1) Maltseva, T. V.; Agback, P.; Repkova, M. N.; Venyaminova, A. G.; Ivanova, E. M.; Sandtrom, A.; Zarytova, V. F.; Chattopadhyaya, J. *Nucleic Acids Res.* **1994**, *22*, 5590−5599.
(2) Egli, M.; Tereshko, V.; Mushudov, G. N.; Sanishvili, R.; Liu, X.; Lewis, F. D. *J. Am. Chem. Soc.* **2003**, *125*, 10842−10849.
(3) Tuma, J.; Richert, C. *Biochemistry* **2003**, *42*, 8957−8965.
(4) Dombi, K. L.; Griesang, N.; Richert, C. *Synthesis* **2002**, 816−824.
(5) Dogan, Z.; Paulini, R.; Rojas Stütz, J. A.; Narayanan, S.; Richert, C. *J. Am. Chem. Soc.* **2004**, *126*, 4762−4763.
(6) Al-Rawi, S.; Ahlborn, C.; Richert, C. *Org. Lett.* **2005**, *7*, 1569−1572.
(7) Marshall, E. *Science* **2004**, *306*, 630−631.
(8) Plutowski, U.; Richert, C. *Angew. Chem.* **2005**, *117*, 627−631.
(9) Mokhir, A. A.; Richert, C. *Nucleic Acids Res.* **2000**, *28*, 4254−4265.
(10) (a) Altman, R. K.; Schwope, I.; Sarracino, D. A.; Tetzlaff, C. N.; Bleczinski, C. F.; Richert, C. *J. Comb. Chem.* **1999**, *1*, 493−508. (b) Mokhir, A. A.; Tetzlaff, C. N.; Herzberger, S.; Mosbacher, A.; Richert, C. *J. Comb. Chem.* **2001**, *3*, 374−386. (c) Mokhir, A. A.; Connors, W. H.; Richert, C. *Nucleic Acids Res.* **2001**, *29*, 3674−3684. (d) Dombi, K. L.; Steiner, U. E.; Richert, C. *J. Comb. Chem.* **2003**, *5*, 45−60. (f) Ernst, T.; Richert, C. *Synlett* **2005**, 411−416.
(11) (a) Yamana, K.; Nishijima, Y.; Ikeda, T.; Gokota, T.; Ozaki, H.; Nakano, H.; Sangen, O.; D'Shimidzu, T. *Bioconjugate Chem.* **1990**, *1*, 319−324. (b) Narayanan, S.; Gall, J.; Richert, C. *Nucleic Acids Res.* **2004**, *32*, 2901−2911.
(12) Connors, W. H.; Narayanan, S.; Kryatova, O. P.; Richert, C. *Org. Lett.* **2003**, *5*, 247−250.
(13) Kryatova, O. P.; Connors, W. H.; Bleczinski, C. F.; Mokhir, A. A.; Richert, C. *Org. Lett.* **2001**, *3*, 987−990.
(14) Siegmund, K.; Maheshwary, S.; Narayanan, S.; Connors, W.; Riedrich, M.; Printz, M.; Richert, C. *Nucleic Acids Res.* **2005**, *33*, 4838−4848.
(15) Cummins, L. L.; Owens, S. R.; Risen, L. M.; Lenik, E. A.; Freier, S. M.; McGee, D.; Guinosso, C. J.; Dan Cook, P. *Nucleic Acids Res.* **1995**, *23*, 2019−2024.
(16) Yamana, K.; Mitsui, T.; Yoshioka, J.; Isuno, T.; Nakano, H. *Bioconjugate Chem.* **1996**, *7*, 715−720.
(17) Korshun, V. A.; Stetsenko, D. A.; Gait, M. J. *J. Chem. Soc., Perkin Trans. 1* **2002**, 1092−1104.
(18) (a) Letsinger, R. L.; Chaturvedi, S. *Bioconjugate Chem.* **1998**, *9*, 826−830. (b) Letsinger, R. L.; Zhang, G.; Sun, D. K.; Ikeuchi, T.; Sarin, P. S. *Proc. Natl. Acad. Sci. U.S.A.* **1989**, *86*, 6553−6556. (c) Soutschek, J.; Akinc, A.; Bramlage, B.; Charisse, K.; Constien, R.; Donoghue, M.; Elbashir, S.; Geick, A; Hadwiger, P.; Harborth, J.; John, M.; Kesavan, V.; Lavine, G.; Pandey, R. K.; Racie, T.; Rajeev, K. G.; Röhl, I.; Toudjarska, I.; Wang, G.; Wuschko, S.; Bumcrot, D.; Koteliansky, V.; Limmer, S.; Manoharan, M.; Vornlocher, H.-P. *Nature* **2004**, *432*, 173−178.
(19) (a) Yamana, K; Ohashi, Y.; Nunota, K.; Kitamutra, M.; Nakano, H.; Sangen, O.; Shimidzu, T. *Tetrahedron Lett.* **1991**, *32*, 6347−6350. (b) Hrdlicka, P. J.; Kumar, T. S.; Wengel, J. *Chem. Commun.* **2005**, 4279−4281. (c) Sorensen, M. D.; Petersen, M.; Wengel, J. *Chem. Commun.* **2003**, 2130−2131. (d) Lindegaard, D.; Babu, B. R.; Wengel, J. *Nucleosides, Nucleotides Nucleic Acids* **2005**, *24*, 679−681.

(20) (a) Amirkhanov, N. V.; Chattopadhyaya, J. *J. Chem. Soc., Perkin Trans. 2* **2002**, 271−281. (b) Zamaratski, D. O.; Pradeepkumar, P. I.; Amirkhanov, N.; Chattopadhyaya, *J. Tetrahedron* **2001**, *57*, 593−606. (c) Ossipov, D.; Zamaratski, E.; Chattopadhyaya, J. *Helv. Chim. Acta* **1999**, *82*, 2186−2200. (d) Ossipov, D.; Pradeepkumar, P. I.; Holmer, M.; Chattopadhyaya J. *J. Am. Chem. Soc.* **2001**, *123*, 3551−3562. (e) Pradeepkumar, P. I.; Cheruku, P.; Plashkevych, O.; Acharya, P.; Gohil, S.; Chattopadhyaya, J. *J. Am. Chem. Soc.* **2004**, *126*, 11484−11499.

(21) Puri, N. P.; Zamaratski, E.; Sund, C.; Chattopadhyaya, J. *Tetrahedron* **1997**, *53*, 10409−10432.

(22) (a) Lewis, F. D.; Liu, X.; Wu, Y.; Miller, S. E.; Wasielewski, M. R.; Letsinger, R. L.; Sanishvili, R.; Joachimiak, A.; Tereshko, V.; Egli, M. *J. Am. Chem. Soc.* **1999**, *121*, 9905−9906. (b) Lewis, F. D.; Wu, Y.; Liu, X. *J. Am. Chem. Soc.* **2002**, *124*, 12165−12173. *(*c) Lewis, F. D.; Wu, T.; Liu, X.; Letsinger, R. L.; Greenfield, S. R.; Miller, S. E.; Wasielewski, M. R. *J. Am. Chem. Soc.* **2000**, *122*, 2889−2902. (d) Herrlein, M. K.; Letsinger, R. L. *Angew. Chem., Int. Ed. Engl.* **1997**, *36*, 599−601.

(23) (a) Aubert, Y.; Asseline, U. *Org. Biomol. Chem.* **2004**, *2*, 3496−3503. (b) Asseline, U.; Cheng, E. *Tetrahedron Lett.* **2001**, *42*, 9005−9010.

(24) Balaz, M.; Steinkruger, J. D.; Ellestad, G. A.; Berova, N. *Org. Lett.* **2005**, *7*, 5613−5616.

(25) Huber, R.; Amann, N.; Wagenknecht, H.-A. *J. Org. Chem.* **2004**, *69*, 744−751.

(26) (a) Bommarito, S.; Peyret, N.; Santa Lucia, J. *Nucleic Acids Res.* **2000**, *28*, 1929−1934. (b) Guckian, K. M.; Schweitzer, B. A.; Ren, R. X.-F.; Sheils, C. J.; Paris, P. L.; Tahmassebi, D. C.; Kool, E. T. *J. Am. Chem. Soc.* **1996**, *118*, 8182−8183.

(27) O'Neill, B. M.; Ratto, J. E.; Good, K. L. Tahmassebi, D. C.; Helquist, S. A.; Morales, J. C.; Kool, E. T. *J. Org. Chem.* **2002**, *67*, 5869−5876.

(28) Grünefeld, P.; Richert, C. *J. Org. Chem.* **2004**, *69*, 7543−7551.

(29) Robins, M. J.; Hawrelak, S. D.; Hernandez, A. E.; Wnuk, S. F. *Nucleosides, Nucleotides Nucleic Acids* **1992**, *11*, 821−834.

(30) Karpeisky, A.; Sweedler, D.; Haeberli, P.; Read, J.; Jarvis, K.; Beigelman, L. *Bioorg. Med. Chem. Lett.* **2002**, *12*, 3345−3347.

(31) (a) Vasilyeva, S. V.; Abramova, T. V.; Silnikov, V. N. *Nucleosides Nucleotides Nucl. Acids* **2004**, *23*, 993−998. (b) Zubin, E. M.; Antsypovich, S. I.; Oretskaya, T. S.; Romanova, E. A.; Volkov, E. M.; Tashlitsky, V. N.; Dolinnaya, N. G.; Shabarova, Z. A. *Nucleosides, Nucleotides Nucleic Acids* **1998**, *17*, 425−440. (c) Walcher, G.; Pfleiderer, W. *Helv. Chim. Acta* **1996**, *79*, 1067−1074.

(32) Karpeisky, A.; Gonzalez, C.; Burgin, A. B.; Beigelman, L. *Tetrahedron Lett.* **1998**, *39*, 1131−1134.

(33) (a) Beier, M.; Stephan, A.; Hoheisel, J. D. *Helv. Chim. Acta* **2001**, *84*, 2089−2095. (b) Uhlmann, E.; Engels, J. *Tetrahedron Lett.* **1986**, *27*, 1023−1026. (c) van de Sande, J. H.; Ramsing, N. B.; Germann, M. W.; Elhorst, W.; Kalisch, B. W.; von Kitzing, E.; Pon, R. T.; Clegg, R. C.; Jovin, T. M. *Science* **1988**, *241*, 551−557. (d) Koga, M.; Moore, M. F.; Beaucage, S. L. *J. Org. Chem.* **1991**, *56*, 3757−3759.

(34) Schwope, I.; Bleczinski, C. F.; Richert, C. *J. Org. Chem.* **1999**, *64*, 4749−4761.

(35) Carpino, L. A.; Imazumi, H.; El-Faham, A.; Ferrer, F. J.; Zhang, C.; Lee, Y.; Foxman, B. M.; Henklein, P.; Hanay, C.; Mügge, C.; Wenschuh, H.; Klose, J.; Beyermann, M.; Bienert, M. *Angew. Chem., Int. Ed.* **2002**, *41*, 441−445.

(36) Berlin, K.; Jain, R. K.; Tetzlaff, C.; Steinbeck, C.; Richert, C. *Chem. Biol.* **1997**, *4*, 63−77.

(37) Bleczinski, C. F.; Richert, C. *J. Am. Chem. Soc.* **1999**, *121*, 10889−10894.

(38) Tuma, J.; Connors, W. H.; Stitelman, D. H.; Richert, C. *J. Am. Chem. Soc.* **2002**, *124*, 4236−4246.

(39) Bugaut, A.; Toulme, J.-J.; Rayner, B. *Angew. Chem.* **2004**, *116*, 3206−3209.

(40) Tuma, J.; Paulini, R.; Rojas Stütz, J. A.; Richert, C. *Biochemistry* **2004**, *43*, 15680−15687.

(41) Mosettig, E; van de Kamp, J. *J. Am. Chem. Soc.* **1930**, *52*, 3704−3710.

(42) El-Bayoumy, K.; Desai, D.; Upadhyaya, P.; Amin, S.; Hecht, S. S. *Carcinogenesis* **1992**, *13*, 2271−2275.

(43) Song, X.; Perlstein, J.; Whitten, D. G. *J. Phys. Chem. A* **1998**, *102*, 5440−5450.

(44) Furuta, T.; Torigai, H.; Sugimoto, M.; Iwamura, M. *J. Org. Chem.* **1995**, *60*, 3953−3956.

(45) Yamato, T.; Miyazawa, A.; Tashiro, M. *J. Chem. Soc., Perkin Trans. I* **1993**, 3127−3137.

(46) Oskolkova, O. V.; Saf, R.; Zenzmaier, E.; Hermetter, A. *Chem. Phys. Lipids* **2003**, *125*, 103−114.

(47) Davenport, L.; Shen, B.; Joseph, T. W.; Straher, M. P. *Chem. Phys. Lipids* **2001**, *109*, 145−156.

(48) Bugaut, A.; Bathany, K.; Schmitter, J.-M.; Rayner, B. *Tetrahedron Lett.* **2005**, *4*, 687−690.

(49) Mokhir, A.; Richert, C. Unpublished results.

(50) (a) Wilds, C. J.; Wawrzak, Z.; Krishnamurthy, R.; Eschenmoser, A.; Egli, M. *J. Am. Chem. Soc.* **2002**, *124*, 13716−13721. (b) Zhang, L.; Peritz, A.; Meggers, E. *J. Am. Chem. Soc.* **2005**, *127*, 4174−4175.

(51) Ma, J.-B.; Yuan, Y.-R.; Meister, G.; Pei, Y.; Tuschl, T.; Patel, D. J. *Nature* **2005**, *434*, 666−670.

(52) Hendrickson, T.; Still, W. C. *J. Comput. Chem.* **1990**, *11*, 440−467.

(53) Humphrey, W.; Dalke, A.; Schulten, K. *J. Mol. Graphics* **1996**, *14*, 33−38.

(54) Nicolaou, K. C.; Safina, B. S.; Zak, M.; Lee, S. H.; Nevalainen, M.; Bella, M.; Estrada, A. A.; Funke, C.; Zecri, F. J.; Bulat, S. *J. Am. Chem. Soc.* **2005**, *127*, 11159−11175.

(55) Tetzlaff, C. Ph.D. Thesis, Tufts University, Medford, MA, 2001.

CC060142A